Adaptation for Multi-Antenna Systems

Christopher Ian Phelps

Thesis submitted to the Faculty of

Virginia Polytechnic Institute and State University

in partial fulfillment of the requirements for the degree of

Master of Science

in

Electrical Engineering

R. M. Buehrer, Chair

J. H. Reed

W. H. Tranter

August 3, 2009

Blacksburg, Virginia

Adaptation for Multi-Antenna Systems

Christopher Ian Phelps

Abstract

The problem of managing multi-antenna resources is one of meeting minimum operating constraints while trying to maximize efficiency. For multi-antenna systems, this requires knowledge of the channel parameters such as angle spread and receive SNR, and knowing how the system will perform for each configuration. System performance is, of course, a function of the entire signaling scheme, including the symbol constellation, the FEC code type and rate in addition to the multi-antenna scheme.

Previous attempts to adapt MIMO systems in the presence of varying channel conditions typically focus on characterizing the performance of a limited and predefined set of joint MoDem/CoDec and MIMO configurations over a representative set of channel realizations. Other work has attempted to adapt only the MIMO scheme to varying channel conditions without considering modulation format or the channel code used. Finally, attempts to configure the system through direct BER calculation based on channel conditions were also proposed. These methods suffer the problems of dependence on a limited set of simulated curves which may not account for all channel conditions that a real system might see, not configuring all parameters jointly or implicitly requiring channel state information to be fed back to the transmitter. None of these previous attempts have handled both cases where CSIT is available or not while jointly configuring the MoDem, CoDec and multi-antenna scheme.

This work consists of two parts, focusing on energy efficiency in the presence of unoccupied frequency bands and on spectrally efficient operation under static frequency assignment. Utilizing minimum Euclidean distances of MoDem constellations and the minimum free Hamming distance metrics for channel codes, we develop distance metrics to describe the MIMO schemes which are considered. A minimum required distance is then determined as a function of desired BER and constellation. Based on the unified set of distance metrics, adaptive algorithms can evaluate the total distance of a signaling scheme, including MoDem, CoDec and MIMO scheme, and then calculate a decision metric based on the total distance and the required distance to meet the desired BER.

The proposed system which aims to maximize energy efficiency is able to choose, based on spatial correlation, available channels, CSIT availability, and power amplifier configuration, the appropriate multi-antenna configuration, MoDem and Codec to meet a fixed throughput requirement while maximizing the energy efficiency or robustness of the link. The proposed work assumes that the open channels of a network can be accessed through individually tunable RF chains of the multi-antenna systems. This assumption permits the use of a multi-antenna, multi-channel scheme which sacrifices spatial diversity for frequency diversity. In addition to traditional, single-channel transmit diversity schemes, the adaptive system is also able choose, when more energy efficient, this novel, multi-channel configuration.

When focusing on the maximization of spectral efficiency, a more conventional, single-channel model is assumed. In addition to the distance metrics for single-channel diversity schemes, distance metrics are then developed for spatial multiplexing schemes which take

into account the interaction of spatial correlation, number of antennas and the rate of the channel code. The adaptive system uses the total distance of the joint configuration of MoDem, CoDec and MIMO scheme to calculate a decision metric which indicates whether the configuration will meet the desired BER. From a list of joint configurations which will meet the desired BER, the adaptive system then chooses the one which maximizes the spectral efficiency.

Acknowledgements

First and foremost, I would like to thank Dr. Michael Buehrer. When he agreed to be my advisor, he took a chance on me and gave me the chance to prove myself. He provided me with opportunity, guidance and inspiration, both professionally and personally for which I will always be grateful and in his debt.

I would like to thank Dr. Jeff Reed and Dr. William Tranter. Through our conversations over the past few years, their professional accounts and guidance have helped me to understand the intricacies of the field and increase my appreciation for it. They have both been a source of inspiration and been shining examples of the qualities needed both to be successful and to continue learning from our experiences.

I must thank Dr. Ira Jacobs for being a constant source of inspiration throughout my undergraduate and graduate careers. Most importantly, Dr. Buehrer, Dr. Jacobs, Dr. Reed and Dr. Tranter have all been sources of wisdom and each of them, the personification of integrity.

I would like to thank my parents and brother. While I'm not sure that they ever truly understood what is was that I was so captivated or motivated by, they needed only to know that it was important to me and have always offered unwavering support for my various pursuits.

A special thanks is owed to the staff and students of the MPRG. They've been my friends and some of them have even become as close as a second family. Without them and their support, this experience would be far more lonely and difficult.

Contents

List of Figures

List of Tables

List of Abbreviations

AoA	Angle of Arrival
AoD	Angle of Departure
AS	Angle Spread
AWGN	Additive White Gaussian Noise
BER	Bit Error Rate
BF	(Eigen-) Beamforming
BLAST	Bell Laboratories Layered -Space-Time
CoDec	Code, Decode
CSI	Channel State Information
CSIR	Channel State Information at Receiver
CSIT	Channel State Information at Transmitter
DSA	Dynamic Spectrum Allocation
EbNo	Energy Per Bit to Noise Spectral Density Ratio
FEC	Forward Error Correction
i.i.d.	independent and identically distributed
LLR	Log-Likelihood Ratio
MIMO	Multiple-Input, Multiple-Output
ML	Maximum Likelihood
MLSE	Maximum Likelihood Sequence Estimation
MMSE	Minimum Mean Square Error
MoDem	Modulate, Demodulate
MRC	Maximal Ratio Combining
MTMR	Multiple-Transmit, Multiple-Receive
PA	Power Amplifier
PSK	Phase Shift Keying
QAM	Quadrature Amplitude Modulation
QoS	Quality of Service
SISO	Single-Input, Single-Output
STBC	Space-Time Block Code
STTC	Space-Time Trellis Code
SNR	Signal to noise ratio
SVD	Singular Value Decomposition

Chapter 1

Introduction

The crowding of the electromagnetic spectrum is accelerating. Required data rates per user, the number of users and the mobility of the average user are increasing simultaneously. Consequently, connections and networking are becoming increasingly ad-hoc and user terminals are subject to an increasing amount of interference. Network planning and spectrum allocation, once utilized as a means to effectively share resources and guarantee performance for independent links and separate systems have not only become impractical to manage the increasing number of users given their mobility, but have also become the cause for much of the inefficiency in resource sharing. Unfortunately, the non-deterministic nature of these newer users and networks precludes a method to effectively predict network configurations or manage end-user performance and thus, much of the intelligence that went into planning more static and traditional networks by system designers now must be automated and pushed closer to the users. Meanwhile, Quality of Service (QoS) expectations from the user

are increasing and the traditional model of voice plus data is yielding to more a wider variety of traffic such as real-time video which may also increase the QoS requirements.

The increasing demands and requirements in the presence of these factors and circumstances require that user radios must become more capable, flexible and agile. The end result is that user radios are becoming more complex and as alluded to, the intelligence to manage and configure radio resource complexity must be built-in to assure that the capabilities are effectively used to maximize the radio's performance in unpredictable environments and network topologies.

1.1 Motivation

With the the ongoing research in cognitive radios and other resource management techniques meant to address the increasing bandwidth and QoS requirements of users and networks, the advanced hardware configurations available in nearly all new radios will both enable the solutions to meet these challenges and increase the complexity of the resources to be managed. A next generation system must be both dynamically reconfigurable to tailor its own performance and sufficiently agile to avoid legacy systems and other competing systems which may also be ad-hoc or have mobile nodes.

After the pioneering work by Foschini [11], multi-antenna systems began a period of heavy investigation. Important work by Foschini and Gans [12] and Telatar [38] investigated the limits and capacities of the MIMO channel and the era of multi-antenna systems had officially begun. Simultaneously, Tarokh [37] and Wolniansky [42] had begun their investigations into

practical architectures to leverage the dimensionality of the MIMO channel.

This work addresses the resource management aspect of multi-antenna systems. Being designed into nearly all future radios or existing as part of nearly all new standards, it is well-known at this point that multi-antenna configurations are one way to leverage diversity to improve performance at the obvious expense of both complexity and cost. Multi-antenna resources, as usually configured, are better known as MIMO systems, or Multiple-Input, Multiple-Output, since in single-frequency operation, the resulting channel is a pairwise coupling of transmit and receive antennas which is most easily viewed as a matrix containing the associated channel states for these couplings. We refer to these systems more generally as multi-antenna or Multiple-Transmit, Multiple-Receive (MTMR) [15] systems because the goal of this work is meant to manage these hardware resources in both single-frequency and multi-frequency operation.

In addition to both single-frequency and multi-frequency operation, this work is goal-driven by both aspects of performance, i.e. spectral efficiency under error constraint and energy efficiency under a signaling rate constraint. The complexity problem of managing multi-antenna hardware is not merely one of signal processing, selection or combining, but also of channel state information and of the channel itself. Mobile radios, dynamic environments, duplex modes, feedback capability, power amplifier configuration and antenna array design all affect the channel characteristics or the viable and appropriate hardware configurations. Specifically, in this work we incorporate the effects of spatial correlation as well as transmitter-side availability of Channel State Information or CSIT in the decision rules.

1.2 Overview

In Chapter 2, the the fundamental concepts of small-scale fading are covered and then developed into an overview of the Multiple-Input, Multiple-Output channel. Correlation in the spectral, temporal and spatial domains are discussed as they relate to the concept of diversity mechanisms. The fundamental concept of diversity-capacity trade-off is discussed as it relates to MIMO systems, and as it makes these systems attractive for adaptive operation based on the characteristics of the channel. The basic concepts of transmit-side and receive-side diversity are discussed. MoDem constellation and FEC channel CoDec design considerations are discussed as well as the feedback channel as a means for coordination, configuration, control and information sharing. Finally, specific configurations of the multi-antenna resources are described.

In Chapter 4, a multi-channel approach is used to explore maximization of energy efficiency as the primary objective for MTMR radio links in a network environment with dynamically assigned, channelized spectrum. A novel approach for multi-antenna, multi-channel resource allocation is presented and applied to MTMR links and its performance is evaluated and compared to traditional, single-channel MIMO diversity schemes. Finally, metrics are developed to predict the performance of both the single-channel and multi-channel diversity schemes and integrated into an adaptive algorithm that switches multi-antenna modes to improve spectral efficiency given varying network and channel conditions relative to any single transmit diversity scheme.

A more traditional objective is explored in Chapter 5 as performance is characterized

for a variety of MIMO diversity and multiplexing schemes and transformed into a set of metrics for maximal spectral efficiency adaptation for MIMO systems. A novel approach is developed to create a set of metrics which closely predicts the performance of the various schemes which is both simple and attractive for implementation. The approach does not rely on storing BER curves, fixed switching points or calculating the probability of bit error at run time. The proposed scheme jointly configures MoDem constellation, FEC CoDec and MIMO scheme in response to spatial correlation and SNR. The metrics are integrated into an adaptive algorithm to show maximum spectrum efficiency over varying channel conditions while meeting a BER constraint.

Finally, in Chapter 6, conclusions, future work and the impact of the proposed work are discussed.

Chapter 2

Background

2.1 Small-Scale Fading

Before the discussion of signaling techniques used in the MIMO channel, the mechanisms which describe it must first be covered. Small-scale fading is the result of multipath propagation in the wireless channel. Multiple, non line-of-sight (NLOS) reflections arriving at a point in space are summed incoherently and the resulting amplitude and phase of the signal is a result of the number of paths by which reflections propagate from source to destination, the reflectivity of the objects which are in the path and the path lengths. If there are a large number of paths with roughly equal amplitude, the summed signal is a complex Gaussian random variable having an amplitude which is a Rayleigh random variable. Independent envelope values are often created by means of a complex Gaussian random variable and temporally-correlated samples are sometimes modeled using the Jakes model [17].

2.1.1 Spectral, Spatial and Temporal Correlation

Correlation between samples of a fading envelope can occur within each of the domains in which a signal exists, those being time, frequency and space. The level of correlation between samples depends on the distance between samples, the signal characteristics as well as the dynamic nature of the environment, the source and the destination.

Due to the effects of multipath on combined with mobility, an effect known as Doppler Spread is observed. Coherence Time is the time domain dual of Doppler Spread and gives a method for measuring the time for which the amplitude of a channel is correlated with itself. In [29], for correlation, $\rho \geq 0.9$ the coherence time is expressed as inversely proportional to the Doppler Spread. Coherence Time gives a measure of time for which the fading envelope remains static between subsequent samples of the channel. Samples of the channel taken at intervals much greater than the coherence time would be assumed to be uncorrelated and thus, independent. In Equation 2.1, this relationship is estimated for rapidly fluctuating channels.

$$T_c \approx \frac{1}{f_m} \tag{2.1}$$

In [32], an expression is given relating Coherence Time and Doppler Shift for more slowly varying channels where $\rho \geq 0.5$ and where f_m is the maximum Doppler shift.

$$T_c \approx \frac{9}{16\pi f_m} \tag{2.2}$$

In the time domain, the path lengths over which the multiple paths propagate will nat-

urally arrive at a point in space with delays proportional to the length of the path. This effect is characterized as Delay Spread and is a measure of the time between the arrivals of paths with power above a threshold. The frequency domain dual of Delay Spread is known as Coherence Bandwidth and gives a measure of bandwidth for which a signal could be assumed to experience correlated (frequency-flat) fading. Samples in frequency separated by less than the coherent bandwidth could assumed to be nearly equal or at least strongly correlated, while samples at distances greater than the coherent bandwidth results in uncorrelated, independent samples and signals sent with bandwidth exceeding the coherent bandwidth would be said to experience frequency selective fading.

The expression for Coherence Bandwidth where correlation, $\rho \geq 0.9$ is given in [22] where τ is the RMS delay spread as:

$$B_c \approx \frac{1}{50\sigma_\tau} \tag{2.3}$$

For $\rho \geq 0.5$, the expression becomes

$$B_c \approx \frac{1}{5\sigma_\tau} \tag{2.4}$$

Finally, a measure of coherence in the spatial domain must be defined. Coherence Space, as it is sometimes called, is a measure of distance in the spatial domain over which samples of the fading channel can be assumed to be correlated. As a function of wavelength, separation between samples and statistical mean and distribution of the arriving paths, an expression for spatial correlation is given in [3].

The expression below describes the case where the arriving (or departing) paths are

assumed to be distributed normally about a central angle.

$$\rho(d) \approx exp\{j\frac{2\pi d}{\lambda}\sin(\phi)\}exp\{-\frac{(\frac{2\pi d}{\lambda}\sigma\cos(\phi))^2}{2}\} \tag{2.5}$$

And this expression describes the case where the distribution is assumed to be uniformly distributed about a central angle.

$$\rho(d) \approx exp\left(j\frac{2\pi d}{\lambda}\sin(\phi)\right)sinc\left(\frac{2\pi d}{\lambda}\sigma\cos(\phi)\Delta\right) \tag{2.6}$$

Where d is the separation between antennas, λ is the wavelength, ϕ is the central Angle-of-Arrival or Angle-of-Departure (AoA) or (AoD) and σ is the standard deviation of the normal distribution of the AoA or AoD while Δ is the one-sided range of angles from the central angle for the AoA or AoD for paths for the uniform distribution.

2.2 Capacity and Diversity of The MIMO Channel

Depending on the MIMO configuration, there is an inherent capacity-diversity trade-off. Essentially, the degrees of freedom provided by the MIMO channel provide dimensions by which diversity is obtained through transmission of versions of the desired symbols or capacity through simultaneous, parallel and separable symbols can be transmitted. In this regard, a system can be configured to have either diversity gain for improved energy efficiency or capacity gain for improved spectral efficiency. With this view, a MIMO system's capacity-diversity trade-off now resembles the familiar AWGN, SISO channel whose limits are bounded by the well know Shannon capacity curve and whose relationship between spectral efficiency and energy efficiency is informed by this relationship. At opposite ends of the

spectrum, the diversity-only transmission is sometimes called 'scalar transmission' while the capacity maximizing transmission is sometimes referred to as 'vector' transmission.

The MIMO channel results from the coordinated usage of multiple sources and destinations over the same fading channel. A result of the multiple sources and destinations is multiple points from which to observe, sample or witness the fading phenomenon. The ability to observe the same channel from different points results in the fundamental concept of dimensionality. In general, degrees of dimensionality are increased when more than one observation is made of the same phenomenon within any of the domains in which the phenomenon exists. Specifically, signal diversity is attainable when the same signal can be observed at different points in time, frequency or space. Capacity can be improved through the projection of different signals onto the dimensions within the time, frequency or spatial domains. The degree of dimensionality is proportional to the distance between observation points in the domain in which they are made. Essentially, dimensional maximization occurs when the observation points are uncorrelated and independent. Sampling in time at intervals greater than the Coherence Time, in frequency at intervals greater than the Coherence Bandwidth or in Space at intervals greater than the Coherence Space will result in maximum dimensionality.

In this work, a narrow band signal model is assumed, thus the Coherence Bandwidth is assumed to be greater than the bandwidth of the signal. This assumption is common and one of simplification that allows a flat-fading channel response assumption. The following expression is for a MIMO channel matrix at time instant n where $\tilde{h}_{ij}$ is the complex gain

between receive antenna i and transmit antenna j.

$$\mathbf{H}(n) = \begin{bmatrix} \tilde{h}_{11}(n) & \tilde{h}_{21}(n) & \dots & \tilde{h}_{1N_t}(n) \\ \tilde{h}_{21}(n) & \tilde{h}_{22}(n) & \dots & \tilde{h}_{2N_t}(n) \\ \vdots & \vdots & \ddots & \vdots \\ \tilde{h}_{N_r1}(n) & \tilde{h}_{N_r2}(n) & \dots & \tilde{h}_{N_rN_t}(n) \end{bmatrix} \tag{2.7}$$

Where N_t and N_r denote the number of transmitting and receiving elements, respectively.

Expressions for MIMO channel capacity are given in [15], for two distinct cases, each with two sub-cases. In the first case, the MTMR system does not have or does not utilize CSIT and the expressions below give capacity for the sub-cases when the number of transmitting antennas (N_t) is greater than or equal to the number of receive antennas (N_r), and when the number of receive elements equals or outnumbers the number of transmit antennas.

$$C = \mathbf{E}[\log_2\{\det(\mathbf{I}_{N_r} + \frac{\rho}{N_t}\mathbf{H}\mathbf{H}^\dagger)\}]bps/Hz \tag{2.8}$$

when $N_t \geq N_r$.

$$C = \mathbf{E}[\log_2\{\det(\mathbf{I}_{N_t} + \frac{\rho}{N_r}\mathbf{H}^\dagger\mathbf{H})\}]bps/Hz \tag{2.9}$$

when $N_t \leq N_r$.

These equations are for systems that transmit with equal power from each of the transmitters and are equivalent when $N_t = N_r$, as in the case of symmetric MIMO links. For operation without CSIT, $/rho$ is the average SNR.

When CSIT is available, the MIMO capacity is expressed as the sum of the capacities taken over the eigenmodes of the channel.

Here, λ_i is the ith eigenvalue of $\mathbf{HH}_{\dagger}$.

$$C = \mathbf{E}[\sum_{i=1}^{N_r} \log_2(1 + \frac{\rho_i}{N_t}\lambda_i)]bps/Hz \tag{2.10}$$

when $N_t \geq N_r$.

$$C = \mathbf{E}[\sum_{i=1}^{N_t} \log_2(1 + \frac{\rho_i}{N_r}\lambda_i)]bps/Hz \tag{2.11}$$

when $N_t \leq N_r$.

Again, these last two expressions become equivalent in the case of symmetric MIMO links. With full CSIT, however, the MIMO channel can be treated as a set of parallel and interference-free SISO channels through decomposition, also allowing the system to allocate power across the sub-streams according to their respective gains. Therefore, $/rho_i$ in this case is the SNR for the i^{th} sub-stream. This approach allows for further capacity maximization through power allocation and rate adjustment on a per sub-stream basis.

For both cases with and without CSIT, † is used to denote the Hermitian or complex conjugate transpose of the matrix.

When CSIT is available, a singular value decomposition (SVD) can be used to take advantage of this knowledge to improve performance of the system [39]. The expressions which describe the the SVD and equivalent channel are in Equations 2.12, 2.13, 2.14 and 2.15, below.

The expression for an SVD is given below.

$$\mathbf{H} = \mathbf{U}\mathbf{\Sigma}\mathbf{V}^{\dagger} \tag{2.12}$$

The singular values are essentially the a measure of the gains of the equivalent channels after decomposition of the MIMO channel.

$$\mathbf{\Sigma} = diag(\sigma_1, \sigma_2, ..., \sigma_{N_t}) \tag{2.13}$$

The left unitary matrix is used to weight and coherently detect incoming signals at the receiver.

$$\mathbf{U} = [\tilde{\mathbf{u}}_1, \tilde{\mathbf{u}}_2, ..., \tilde{\mathbf{u}}_{N_r}] \tag{2.14}$$

The right unitary matrix is used to weight and co-phase the transmitted symbols.

$$\mathbf{V} = [\tilde{\mathbf{v}}_1, \tilde{\mathbf{v}}_2, ..., \tilde{\mathbf{v}}_{N_t}] \tag{2.15}$$

2.2.1 Transmit-side Diversity

The MIMO channel matrix is a generalization of the case with both transmit- and receive-side diversity, however, looking specifically at the case where there are multiple transmit elements and only one receive element, the MIMO channel matrix collapses into the degenerate case known as the MISO channel matrix.

$$\mathbf{H}(n) = \begin{bmatrix} \tilde{h}_1(n) & \tilde{h}_1(n) & \dots & \tilde{h}_{N_t}(n) \end{bmatrix} \tag{2.16}$$

In any multi-antenna system with multiple transmit antennas, there are three primary types of transmit diversity.

2.2.1.1 Transmit Selection

Transmit selection diversity is a scheme by which the only one element from the transmit array is used as any time instance. At first, this scheme does not seem to provide diversity, however, the diversity results from the selection of the transmit element. The selection of the element can either be arbitrary, configured by feedback from the receiver or chosen based on some channel information available to the transmitter, but not necessarily full CSIT. A typical assumption for transmit selection is the capability of the total power available to the transmit array can be combined and used on any single element of the array or $P_{total} = \sum_{j=0}^{N_t-1} P_j$ and $\mathbf{P}_{tx} = [0, 0, ...P_{total}, ...0]$

2.2.1.2 Equal-power transmission

The transmit diversity scheme most often employed for systems without CSIT utilizes equal power allocation across all of the transmitting elements. In much of the literature, equal power allocation is implicit in discussions of transmit diversity. This power allocation strategy is also implicit in the development of Space-Time Codes (STC) including Space-Time Block Codes (STBC) and Space-Time Trellis Codes (STTC). The power allocation profile obeys $P_{total} = \sum_{j=0}^{N_t-1} P_j$ and $P_j = \frac{P_{total}}{N_t}, j = 1, 2, ..., N_t - 1$.

2.2.1.3 Maximal Ratio Transmission

Finally, when full CSIT is available and the total transmit power is available to allocate across the transmit array in an unequal manner, an SVD (Equation 2.12) is used to de-

termine the complex weighting vector for the transmitted symbols. The complex weighting vector is actually just the column of the right unitary matrix corresponding to the maximum singular value of the channel matrix or Equation 2.15. This complex-valued weighting vector normalizes the overall transmit power but weights and co-phases according to the eigenmodes of the matrix. While the term Maximal Ratio Transmission is used to imply its duality to Maximal Ratio Combining, Eigenbeamforming is the more commonly used term to describe this transmit-side diversity scheme. For MRT or BF, the only constraint on power allocation is normalized $P_{total} = 1$ thus $1 = \sum_{j=0}^{N_t-1} P_j$ with $0 \leq P_j \leq 1, j = 1, 2, ..., N_t - 1$

2.2.2 Receive-side Diversity

To illustrate receive-side diversity, when a multi-antenna system has multiple antennas at the receiver only, the MIMO channel becomes the degenerate case known at the SIMO channel, as shown below.

$$\mathbf{H}(n) = \begin{bmatrix} \tilde{h}_1(n) \\ \tilde{h}_2(n) \\ \vdots \\ \tilde{h}_{N_r}(n) \end{bmatrix} \tag{2.17}$$

Again, there are three primary types of combining commonly referred to in the literature. Square-law combining is an example of a practical type of combining rule for implementation that is not included, but commonly used in practice. While receive-side diversity schemes have diversity mechanisms and gains analogous to their transmitter-side duals, when summing multiple samples, they have the added benefit in that combining multiple noisy samples

also help to improve SNR which is called receive array gain. In the following, γ denotes SNR.

2.2.2.1 Selection Combining

Selection combining, strictly speaking, does not combine received signals, but chooses the received version of the signal which maximizes SNR. It is analogous to transmit selection in that the diversity is a result of the selection of the appropriate element. Selection combining is potentially more economical than other receive combining techniques since a single RF chain can switch its input among multiple antennas. The receive SNR is expressed below.[15]

$$\gamma_{sc} = \max\{\gamma_1, \gamma_2, ..., \gamma_{N_r}\} \tag{2.18}$$

2.2.2.2 Equal Gain Combining

Equal gain combining is a true combining technique requiring RF chains for each of the receive antenna elements, where the received signals are co-phased, equally weighted and summed coherently. Like selection combining, it is sub-optimal but avoids some practical issues that are involved in the optimal receive combining techniques. The expression for post-combining SNR is given below. [15]

$$\gamma_{egc} = \frac{[\sum_{i=0}^{N_r-1} |\tilde{h}_i|]^2}{[\sum_{i=0}^{N_r-1} \sigma_i^2]} \tag{2.19}$$

2.2.2.3 Maximal Ratio Combining

Maximal Ratio Combining is the optimal receive combining technique. Like equal gain combining, it requires RF chains for each of the receive antennas. Unlike equal gain combining,

an additional variable gain stage is included in each RF chain and before summing, the gain weights are set according to the respective channel gains. After weighting and co-phasing, the received signals are summed coherently resulting in a post-combining SNR which is equal to the sum of the respective SNRs. The expression is given below. Further work for MRC in Nakagami fading is presented in [1].

$$\gamma_{mrc} = \sum_{i=0}^{N_r-1} \gamma_i \tag{2.20}$$

2.3 MoDem, FEC CoDec and Feedback Configurations

2.3.1 Modulation and Demodulation

For the work considered, four commonly used MoDem constellations are used: QPSK, 8-PSK, 16-QAM and 64-QAM.

At the time of demodulation, (with the exception of BLAST detection), after the received symbols are de-mapped to their ML transmitted symbols, soft bit values are generated for each bit position per symbol as in [28]. Once soft bit values are generated, and since CSIR is assumed for space-time decoding, side information (SI) in addition to noise variance are used to generate bit-wise Log-Likelihood Ratios (LLR) values according to [43]. In [20], the authors investigated soft metric generation for higher order constellations given a fading channel or Generalized LLR (GLLR) and in [41], the authors considered the effects of channel estimation error on performance. The final, compact bit-wise LLR values for a fading channel using SI are computed as below.

$$\Lambda = \ln \sum_{s^+ \in \{s:c_k=+1\}} \exp\left(-\frac{|x-\alpha s^+|^2}{\sigma_n^2}\right) - \ln \sum_{s^- \in \{s:c_k=-1\}} \exp\left(-\frac{|x-\alpha s^-|^2}{\sigma_n^2}\right) \tag{2.21}$$

Where α is the channel gain, s is the transmitted symbol and c_k is the bit at position k within the transmitted symbol.

An important metric used to predict the performance of various modulation formats is the Euclidean distance between symbols in the constellations. Since symbols are most likely to be erroneously de-mapped to the nearest neighbors within the constellation, it is these nearest neighbor inter-symbol distances which can be used to very accurately predict the approximate symbol error performance of these uncoded modulation formats. When reflected binary coding, or Gray coding is used to map bits to symbols, the approximation for symbol error performance can then be used to predict bit error performance.

The minimum Euclidean distances between symbols for the considered constellations were found after normalizing the average signal power to unity. This method allows for a more direct comparison of the constellations without the need to define the received symbol energy. This method for computing the distance metrics is also important because is allows the variables under the radical in the Q-function to be treated separately. Ultimately, because it is desirable to choose constellations based on gains and SNR, this method does not require the actual Euclidean distance to be recalculated as SNR and channel conditions fluctuate.

Expressions to estimate the expected BER for these constellations in an AWGN channel

Table 2.1: Average Power Normalized Minimum Euclidean Distances

MoDem Constellation	d_{min}
QPSK	2
8-PSK	0.765
16-QAM	0.6325
64-QAM	0.3086

are given in Equations 2.22, 2.23, 2.25 and 2.26.

$$P_{b,QPSK} = Q\left(\sqrt{\frac{d_{min}^2}{2}\frac{E_b}{N_o}}\right) \tag{2.22}$$

$$P_{b,8-PSK} \approx \frac{1}{\log_2(M)} 2Q\left(\sqrt{\frac{d_{min}^2}{2}\frac{\log_2(M)E_b}{N_o}}\right) \tag{2.23}$$

$$\begin{aligned} P_{b,16-QAM} \approx & \\ & \frac{1}{\log_2(M)}\frac{1}{4}2Q\left(\sqrt{\frac{d_{min}^2}{2}\frac{\log_2(M)E_b}{N_o}}\right) + \\ & \frac{1}{\log_2(M)}\frac{1}{2}3Q\left(\sqrt{\frac{d_{min}^2}{2}\frac{\log_2(M)E_b}{N_o}}\right) + \\ & \frac{1}{\log_2(M)}\frac{1}{4}4Q\left(\sqrt{\frac{d_{min}^2}{2}\frac{\log_2(M)E_b}{N_o}}\right) \end{aligned} \tag{2.24}$$

$$P_{b,64-QAM} \approx \tag{2.25}$$
$$\frac{1}{\log_2(M)}\frac{1}{16}2Q\left(\sqrt{\frac{d_{min}^2}{2}\frac{\log_2(M)E_b}{N_o}}\right) +$$
$$\frac{1}{\log_2(M)}\frac{3}{8}3Q\left(\sqrt{\frac{d_{min}^2}{2}\frac{\log_2(M)E_b}{N_o}}\right) +$$
$$\frac{1}{\log_2(M)}\frac{9}{16}4Q\left(\sqrt{\frac{d_{min}^2}{2}\frac{\log_2(M)E_b}{N_o}}\right)$$

2.3.2 Forward Error Correction and Interleaving

Made attractive by is familiarity, relative simplicity and good performance, convolutional coding with Viterbi decoding is a commonly implemented channel code that encodes the incoming data stream, adding redundancy and memory. From [27], the free-distance maximizing generator polynomials and puncturing matrices can be found. For this work, the convolutional code is based on the $K = 8$ generators and rates where $R_c \geq 1/2$, the optimal puncturing matrices from [27], based on $R_c = 1/2$ codes are used. Additionally, zero-state forcing is used, but the length of the incoming data stream is made long enough so that no additional coding gain from this termination method is realized. While the error correction capabilities of convolutional codes can not be predicted on a codeword-by-codeword basis as they can for block codes, for convolutional codes, asymptotic performance gains can be approximated by knowing the rate and the Hamming distance of the lowest weight, non-zero divergent path through the trellis, known as the free distance or d_{free}. The rates and distances for the codes considered in this work are listed below in Table 2.2.

Table 2.2: $K = 8$, Convolutional Codes and d_{free}

R_c	d_{free}
Uncoded	1
$\frac{3}{4}$	6
$\frac{2}{3}$	7
$\frac{1}{2}$	10
$\frac{1}{3}$	16
$\frac{1}{4}$	22
$\frac{1}{6}$	34

Since convolutional codes are designed to work for AWGN channels, they must be handled with special care on fading channels or when modulated symbols experience different channel gains during transmission such as in channels where the coherence time is less than the time to transmit a codeword or when multiplexed sub-streams are transmitted over quasi-static channels. For this reason, a standard block-interleaver is inserted between the channel encoder and the symbol mapper. For this work, the block interleaver has the same number of elements as the coded bit stream and serves to randomize the received, coded bits before decoding. Assuming that the interleaver depth is greater than the coherence time of the channel, fading induced errors will appear to be more noise-like to the decoder and decrease

the likelihood of decoding error.

2.3.3 Feedback Channel for Closed-Loop Operation

For adaptive systems, it is implicit that some sort of feedback mechanism is employed to adjust operating parameters in response to changes in environment, performance and QoS requirements and it is often assumed that this feedback is both error-free and requires negligible bandwidth and power. While this assumption is of course for convenience only and does not reflect reality, this standard assumption leads to a fair comparison with the majority of research on adaptive systems.

Close-Loop operation allows some variable amount of information to be sent back to the transmitter about configuration, performance or the channel. In an ARQ scheme, for example, the receiver is implicitly sending information to the transmitter about the performance of the current configuration. At the other extreme, the feedback channel may send back the complete channel matrix to the transmitter. In between these two examples, the receiver may send back only an entry from a codebook that corresponds to a particular configuration, or some statistical information about the channel, or in lieu of the full channel matrix, it may send back only the eigenvectors which it would like the transmitter to use.

The speed of the feedback channel relative to the Coherence Time of the channel is also an important parameter to consider. In a system with a feedback channel which updates slower than the speed of the channel variation, configuration must be done on a time-averaged basis. For example, while the fading channel might be varying at a rate faster than the feedback

channel as a result of environmental changes, the variation of the covariance matrices describing the correlation at the transmitter and receiver antenna arrays is likely to be static or changing slowly relative to the speed of the feedback channel. Under these circumstances, the adaptive system must take a statistical approach to adaptation.

2.3.4 Frequency and Time Duplexing Operation

Two potential scenarios help to inform assumptions about the availability of CSIT and the feedback mechanism. In a frequency-duplexed system, the upstream and downstream components of a link are at different frequencies and thus, will experience different propagation effects. Because of this, frequency-duplexed systems are reliant on explicit feedback when the duplex frequencies are separated by more than the coherent bandwidth of the channel and thus, eliminating the possibility that the propagation effects and channel are correlated. In time-duplexed operation, the upstream and downstream components share the same bandwidth, and when the duplexing operation happens more quickly than the coherence time of the channel, reciprocity is the conventionally made assumption, which allows both nodes to have full CSIT when it is their turn to transmit. When the assumption about the duplexing duty cycle relative to coherence time can not be made, explicit feedback is required as it is in frequency-duplexed operation, because the CSIT measured by reciprocity will become stale too quickly to be used.

2.4 Multi-Antenna Configurations

2.4.1 Parallel SISO with Multi-Channel DSA

In Chapter 4, the novel scheme which is proposed sacrifices receive array gain and spectral efficiency when the sub-streams are frequency-multiplexed over what are assumed to be non-contiguous, narrow-band channels, subject to sufficient frequency selectivity to allow the assumption that the MIMO channel realization is i.i.d from frequency band to frequency band. Additionally, a simplifying assumption is made that allows the spatial correlation and covariance matrices describing the antenna arrays to remain constant even though that realistically, the actual spatial correlation is a function of wavelength. It is assumed that the maximum difference in frequency between multiplexed sub-streams is small enough that the change in wavelength has reasonably negligible effect on the spatial correlation between antennas within the arrays.

The multi-channel DSA mechanism, which will be described, is a novel approach to multi-antenna, multi-channel resource allocation and is used to select the frequencies from a given channel realization. The DSA scheduler chooses N_t channels to use from the N_c available channels with which it is presented. As such, the system implicitly uses all transmit antennas available, provided that $N_r \geq N_t$ and $N_c \geq N_t$.

2.4.2 Transmit Diversity with and without DSA

In Chapter 4, fair comparisons between diversity approaches must be made. For this reason, a simple, single-channel DSA was created for each traditional transmit diversity scheme to evaluate the multi-frequency MIMO channel realization and choose the single frequency which maximizes the realized diversity gain for each particular scheme. In Chapter 5, in the absence of multiple frequency channels, there is no DSA required.

For this work, Eigenbeamforming (or sometimes MRT), STBC, and Transmit selection are evaluated. Of these four, STBC is the only approach that is allowed under an equal power constraint, while all others require a more flexible PA assumption. Additionally, while Eigenbeamforming requires full CSIT or the maximum eigenvector to be supplied by the the receiver through the feedback channel, transmit selection requires the transmitter index in addition to the codebook configuration index.

The history of space-time coded transmit diversity schemes is rather interesting and began with [4] where design criteria were developed for space-time coding. The authors defined Rank and Determinant criteria for STCs. Because the authors were investigating a combined approach to channel coding and spatial diversity, the determinant criteria describes the potential coding gain of the space-time codeword while the rank criteria describe the potential diversity gain of the space-time codeword. In [30], the same group of researchers described the class of combined channel and space-time code known as Space Time Trellis Codes or STTC. In the same spirit as Trellis Coded Modulation, the codeword, constellation mapping and transmitter mapping was done jointly, as was the detection, de-mapping and

decoding operation at the receiver. Finally, in [37], this group of researchers released the generalization of STTCs including design criteria. Out of nowhere it now seems, in [2], the author proposed a much simpler transmit diversity scheme now named the Alamouti scheme, after its author. This class of simpler, memoryless and linear STC is known as Space-Time Block Codes, or STBC. Though this proposed scheme was simple, did not combine channel coding and was initially limited to only two transmit antennas, it seemed to have an effect on the researchers working on STTCs, as this original group, in [34] and [35] generalized STBCs and presented some improvements. In [13], the authors proposed an improved version of the sporadic codes for 3 and 4 transmit antennas presented in [35]. Finally, in [36], the authors proposed a class of Layered Space-Time transmission based on STTC component codes, in a effort to explore the capacity gain regime of the MIMO channel.

As is always the case with coding of any kind, the performance relative to rate was heavily investigated, as researchers did not initially know the rates at which STBCs could be encoded. The Alamouti scheme is the only full rate complex, orthogonal STBC, or CO-STBC in existence and it was not yet known how the upper bound on rate related to the number of transmit antennas participating in the transmit diversity scheme. In [40], it was proven that the rate achieved by the sporadic codes for 3 and 4 transmit antenna systems of $R_c = \frac{3}{4}$ was the maximum achievable for transmit arrays of this size. Finally, the general rate limit as a function of N_t was proven in [23] and finally, in [33], the required block length to achieve maximum rate was investigated.

Though only complex orthogonal STBCs are considered here, there are of course quasi-

orthogonal STBCs which sacrifice linearity for rate maximization and of course, STBCs which are real only, but as a result are not suitable to complex constellations, thus limiting their attractiveness for most systems.

2.4.3 Spatial Multiplexing

In Chapter 5, the capacity-diversity trade off is investigated. In addition to the transmit diversity schemes, multiplexing schemes will be evaluated as well. Without full CSIT, transmit multiplexing is used. In this scheme, sub-streams are sent from each of the participating antennas and detected using Bell Labs Layered Space-Time (BLAST)-type detection. Specifically, a Vertical (V)-BLAST receiver is used with MMSE ordering and cancelation. The original work on V-BLAST, given its name, was performed at Bell Laboratories and can be found in [42], [14], [6] and [10]. This original work attracted a lot of interest. Even now, the work that is being performed to adaptively exploit the capacity-diversity trade off of the MIMO channel has been motivated by the computationally attractive detection and decoding methods for both the diversity- and capacity- enhancing BLAST-type systems. While the MMSE V-BLAST scheme is not the optimal in the sense that it does not use ML detection, it was created specifically to avoid the tremendous complexity required for true ML detection of transmit multiplexed streams and while achieving performance very close to the ML detector, and far superior to a Zero-Forcing (ZF) ordering and nulling V-BLAST receiver. Additionally, the MMSE V-BLAST detector is able to achieve this level of performance with only a small increase in computational complexity over the ZF receiver.

With full CSIT, eigenmode-multiplexing is used for spatial multiplexing. For this arrangement, full CSIT or the eigenvectors corresponding eigenmodes of the channel must be available to the transmitter.

Finally, for both spatial multiplexing schemes, the number of sub-streams is allowed to be reduced in response to channel variation. In the BLAST-type system, the feedback channel carries with it, in addition to the usual configuration information, the subset of transmitters to be used in the case of reduced sub-stream transmit multiplexing. The subset is generated from the ordered detection and cancelation operation at the receiver. Since the performance is dominated by the last sub-stream to be detected, the transmitters to be used will correspond to the first transmitters that are to be detected. In the case of eigenmode multiplexing, the transmitter decides how many of the eigenvectors to transmit on based on the error dominating performance of the weakest eigenmode.

Chapter 3

Previous Work

A search for previous work in the area of adaptive multi-antenna systems yields a rich and growing body of work. Of the more recent work which will be briefly covered here, previous attempts must first be categorized by assumptions made by the authors about the availability of Channel State Information to the Transmitter (CSIT) for a given MIMO link. At one end of the spectrum, full CSIT is assumed, and by implication, the assumption that the Power Amplifier (PA) configuration of the transmitter allows the total power available to be allocated unequally amongst the participating transmitting elements. With CSIT, or eigenvector knowledge at the transmitter, traditional transmit diversity and transmit multiplexing schemes are possible as well as more complex and efficient schemes that transmit stream(s) along the eigenmodes of the channel.

At the other end of the spectrum, CSIT is not assumed, eliminating the possibility of eigenmode transmission. Under this assumption, traditional transmit diversity and transmit

multiplexing schemes are possible, optionally augmented by the flexibility of the PA in allocating power to the participating transmit elements, and increasing the number of transmit diversity options.

Along with the assumptions about transmitter-side channel knowledge, previous work also must be compared in terms of the main objective for optimization, the signaling parameters which are configured by the adaptive schemes, and their ability to configure themselves for a channel, taking into account the degree of spatial correlation.

There are three notable works which aim to adapt the MIMO scheme to channel and link conditions while assuming CSIT. In [44], CSIT allows the transmitter to perform an SVD and either adjust the number of eigenmodes or to adjust the power to each of the streams. For this work, the MoDem uses 16-QAM, but no FEC CoDec is used.

In a second work [31], which also assumes CSIT, the MoDem constellation is allowed to vary between BPSK, 4-QAM (QPSK) and 16-QAM. In this work the variable constellation size allows the transmitter to compensate for the relative gains of the eigenmodes. As in the [44] though, channel coding is ignored.

Finally, in [21], the authors propose a unique combination of Diagonal BLAST and Vertical BLAST. For a 4x4 system with CSIT, the authors propose that the system vary the level of redundancy of transmitted symbols within the Space-Time encoded blocks. While the authors claim that the system converges to D-BLAST when symbol redundancy (diversity) is maximized and V-BLAST when rate is maximized, they are using an MMSE ordered SIC method to separate the transmitter-multiplexed streams and then recombine depending on

the diversity-multiplexing mode the system has chosen, thus the system does not truly converge to D-BLAST when the system is transmitting with maximum space-time redundancy. Regardless, the system entirely neglects the gains that are possible with CSIT and since they are limited to symbols mapped from a QPSK constellation, they also ignore channel coding in their system.

In these first three examples, the main objective for adaptation was to maintain an acceptable BER while maximizing the overall spectral efficiency of the system. However, in none of these examples do the authors jointly adapt MoDem constellation, FEC CoDec and MIMO scheme.

There is one example of work where CSIT is not strictly assumed, but the eigenvectors of the channel are updated at the transmitter by way of the feedback channel. In terms of performance, the system found in [18] should be compared, appropriately, to the systems where CSIT is assumed. In this system, groupings of the transmit antenna array participate in sub-streams which are spatially multiplexed. When there is one sub-stream, this is equivalent to Eigenbeamforming and when the number of sub-streams is equal to the number of participating elements in the transmit array, the system is equivalent to a BLAST-type system. In this work, the issues involved in adaptation of constellation or FEC is not addressed and the main objective is to maximize spectral efficiency for a given channel and receive SNR.

Moving on to systems where CSIT is not assumed, there is somewhat more interest since there is potentially more applicability given the practical considerations and complication of

maintaining channel information at the transmitter.

One of the most prominent, yet simple examples of adaptation for a MIMO system without CSIT is [16]. For this system, the main objective is to minimize the BER for a fixed spectral efficiency and regardless of received SNR. In this work, the system switches between full diversity and full multiplexing modes with appropriate constellation sizes chosen for each mode which allow the fixed spectral efficiency constraint. While the MoDem is chosen for each of the two modes, the constellation size is not varied other than when the mode multi-antenna scheme is switched. Channel coding is not considered. The novel contribution of this paper, however, is the use of the Demmel Condition Number as a metric for estimating the spatial selectivity of the channel and thus the appropriate multi-antenna scheme while considering the minimum Euclidean distance of the respective MoDem constellations. A later adaptation of [16], by the same authors was presented in [7] which considered the effects of correlated MIMO channels and at least one project was developed to measure the Demmel condition number and characterize various types of MIMO channels [19].

In [26] sub-streams were strictly spatially multiplexed while the adaptive component of the system determined the number of sub-streams and from which subset of elements of the transmit array. This work then went on to evaluate both BLAST-type detection including ordered interference cancelation and a sequential detection where order of the detection and cancelation were fixed. In both systems, a required spectral efficiency was the main objective and the system was then configured to minimize the BER for the given channel, SNR(s) and required spectral efficiency. With BLAST-type detection, the constellation was the same

across the transmitting elements to meet the required spectral efficiency given the number of participating transmit elements while the number and subset of these elements were determined by the order in which BLAST detection was to occur and by the post-processing SNR. In the system with fixed-order detection and cancelation, bit allocation across all of the transmit elements (up to the number of receive elements) is determined through joint optimization with the post detection SNR after ordered detection and interference cancelation. Implicit to the latter approach is that while all transmit elements are potentially active, the bit allocation may result in transmit element(s) which would result in a sub-threshold SNR for its respective sub-stream post-detection.

In [45] spatially multiplexed sub-streams are received using BLAST-type detection. Unlike ordinary V-BLAST however, a feedback channel is designed to send configuration information about constellation selection for each of the transmitting elements and a power allocation vector. Implicit to this configuration is that the PA is capable of handling such a power allocation. As would be expected with power allocation across the transmit elements and individual constellation selection, this closed-loop system outperforms the standard, open-loop V-BLAST system. Somewhat intuitively, the proposed system also outperforms the standard V-BLAST system by large margins in channels with greater spatial correlation, where diversity and spatial dimensionality are decreased and thus less able to support the full degree of multiplexed streams. Once again, while the constellation is adapted in response to the channel with the objective of reduced BER, channel coding and the number of multiplexed sub-streams are not considered.

Two notable works which attempt to adapt constellation and channel code in addition to MIMO configuration were [5] and [8] which expanded upon [9]. In both cases the configuration of MoDem, CoDec and MIMO scheme was performed jointly based on a look-up table. In the former, spatial correlation is ignored as well as the rank and conditioning of the matrix and adaptation is performed solely in response to SNR fluctuations. In the latter, however, the conditioning of the channel matrix is considered and the look-up table is generated for all combinations of MoDem, CoDec and MIMO scheme for various combinations of SNR and "spatial selectivity" values, where "spatial selectivity" is the Demmel Condition Number for the covariance matrix. Based on a calculated "spatial selectivity" value and average SNR, the receiver configures the transmitter via the feedback channel according to the look-up table. In one of the MIMO configurations however, the required bandwidth for the feedback channel increases as the transmitter requires the dominant eigenvector to perform beamforming.

Finally, the work which by intent is closest to the objective in Chapter 5 is found in [25]. With the main objective of maximizing spectral efficiency while meeting a BER constraint, this work also seeks to be independent of pre-generated look-up tables of switching points. [25] also addresses the issue of joint configuration of MoDem, CoDec as well as MIMO configuration. With two MIMO schemes (beamforming and spatial multiplexing), BER expressions are derived for arbitrary bit-interleaved coded modulation (BICM). Using the covariance matrices for the transmit and receive arrays, the receiver calculates the BER for all possible configurations and chooses the mode which meets the BER operating constraint

while maximizing the spectral efficiency. While this work is very similar to the proposed system, it does not consider reduced-rate multiplexing and requires that the receiver calculate BER which could potentially be computationally intensive.

3.1 Deficiencies of Previous Work Addressed by Proposed Work

The vast majority of the previous work does not deal with joint configuration of the MoDem and CoDec with the MIMO scheme, and most of them ignore reduced-rate multiplexing. This work proposes to address these deficiencies by jointly configuring MoDem, CoDec and MIMO scheme in response to channel characteristics and average SNR.

While there was no multi-channel, multi-antenna work for comparison to Chapter 4, the work which seeks to minimize BER for a fixed spectral efficiency would be the closest. While spectral efficiency is a variable in Chapter 4, the main goal is to choose a configuration which maximizes energy efficiency while overall throughput is fixed.

Chapter 4

Energy Efficiency

4.1 Introduction

Common approaches to multi-antenna adaptation focus on increasing spectral efficiency while meeting an operating constraint such as BER. Spectral efficiency, however, is only one half of the tradeoff that communications engineers may work with. In many real world cases, it may be more desirable to minimize the power required, or to choose a configuration with higher resiliency or robustness to channel variations while achieving a fixed throughput. With multi-antenna systems, it becomes possible to leverage the frequency agility and independently tunable RF chains in combination with unoccupied frequency bands to create multiple, frequency-multiplexed and parallel sub-streams between multi-antenna radios. This configuration, unlike single-band MIMO diversity schemes ordinarily employed with multi-antenna systems, is able to directly sacrifice bandwidth efficiency by using multiple,

though not necessarily adjacent frequency bands to increase energy efficiency by decreasing the overall energy required to transmit at the same aggregate data rate. This approach is analogous to any system which uses bandwidth expansion techniques to improve energy efficiency, though the proposed method requires appropriate resource allocation techniques to assure that the trade-off is beneficial. The proposed work on this configuration shows that under certain channel conditions, this multi-band approach is able to outperform single-band diversity approaches even while accounting for the loss of spatial diversity and receive array combining gain. An important contribution of this work is the scheduling techniques used to arrive at these conclusions which may also have application to other resource allocation problems.

4.2 System Description

In a network environment with a pool of channelized frequency bands used for establishing links between nodes, there will exist bands that are unoccupied for periods of time while links are not utilizing them. A multi-band radio could potentially access these underutilized bands dynamically in order to augment its own performance. In effect, a multi-band approach would potentially capitalize on sparsely populated network environments to either reduce its own power consumption or to improve its link quality. From a flow perspective, a multi-band link would be no different from a single-band link since the overall data rate remains constant. In the proposed system, a multi-antenna, multi-channel approach is considered in addition to traditional, single-band MIMO-based diversity schemes.

The proposed system, consisting of multiple transmit and receive antennas, along with multiple unoccupied channels within the network, is assumed to have CSI for each of the frequencies which is available, either through training sequences or some other network mechanism for channel sounding. It is also assumed that $N_t \leq N_r$ and $N_t \leq N_c$. Based on instantaneous channel measurements, the proposed system is permitted to choose from either a single-band MIMO diversity scheme, or the proposed multi-band scheme. The system will use the set of metrics, which are developed in Section 4.5, to choose the multi-antenna approach which maximizes energy efficiency for a fixed throughput. Given the fixed throughput requirement, the constellation sizes and coding rates are chosen based on the overall throughput requirement and the number of transmit antennas.

Assuming that there are at least as many receive antennas and open frequencies as transmitting antennas, this multi-band configuration, called, Parallel SISO, assigns a receive antenna and open band to each of the participating transmit antennas. The main data stream is then split into sub-streams which are split equally across the multiple parallel SISO channels. Optionally, the main data stream can be channel coded and interleaved across the sub-streams and then recombined at baseband in the receiver. Since no assumptions are made about the adjacency of the multiple bands used for this approach, it is assumed that there is no array combining performed at the receiver. As a result of the frequency-duplexed nature of this link, the sub-streams can assumed to be interference-free. Finally, since the multi-band link is composed of parallel SISO links, traditional equalization techniques can be used on a per-frequency basis, as opposed to the very complex equalization that are required

with single-band MIMO approaches. While this is not the focus of our work, it may be of great interest in terms of practicality and suitability for implementation.

In Tables 4.1 and 4.2 below, the required spectral efficiency is listed for each MTMR configuration in order to achieve the throughput in the left-most column. As can be seen, the multi-band configurations requires a less spectrally efficient MoDem-CoDec combinations when compared to the single-band configurations. When finding combinations of MoDem, CoDec and MTMR configurations for a fair comparison, the configurations used must be realizable based on our MoDem-CoDec codebook that will be developed in Section 5.1, and the MoDem-CoDec combination for both single-band and multi-band configurations should be either both coded or uncoded. In Tables 4.1 and 4.2, the comparable configurations have been highlighted.

For the $2x2$ system in Table 4.1, the full-rate, Alamouti code can be used for the STBC system, so there is no required increase in spectral efficiency due to a space-time coding rate loss. Also, with a $2x2$ system, the Parallel SISO system is able to reduce its spectral efficiency by half compared to the single-band diversity schemes.

In Table 4.2, special attention must be paid to the code rate of the Space-Time Block Code used for systems with four transmit antennas. With a $4x4$ system, since the maximum STBC code rate is $R_c = \frac{3}{4}$, the STBC configuration requires higher spectral efficiency than the other single-band transmit diversity schemes to maintain the same throughput. As was the case for the $2x2$ system, the Parallel SISO configuration can now reduce its spectral efficiency further while maintaining the equivalent throughput. We can see that due to

Table 4.1: Throughput and Spectral Efficiency for MTMR Approaches, 2x2

$Throughput$	BF	$SelTX$	$STBC$	$Psiso$
$bps/(sub-streams \times Hz)$	bps/Hz	bps/Hz	bps/Hz	bps/Hz
0.33	0.33	0.33	0.33	0.17
0.5	0.5	0.5	0.5	0.25
0.67	**0.67**	**0.67**	**0.67**	**0.33**
1	**1**	**1**	**1**	**0.5**
1.33	**1.33**	**1.33**	**1.33**	**0.67**
1.5	1.5	1.5	1.5	.75
2	2	2	2	1
2.25	2.25	2.25	2.25	1.13
2.67	**2.67**	**2.67**	**2.67**	**1.33**
3	**3**	**3**	**3**	**1.5**
4	**4**	**4**	**4**	**2**
4.5	**4.5**	**4.5**	**4.5**	**2.25**
6	6	6	6	3

the choices in the MoDem-CoDec configuration and the space-time coding rate, that the number of valid comparisons that maintain the same throughput and are either all coded or all uncoded have been vastly reduced and that the comparisons would have to be done at different levels of throughput for a comparison of Beamforming, TX Selection and Parallel SISO as they would have to be for a comparison between STBC and Parallel SISO. While the comparisons were investigated to validate the work in this chapter, the $4x4$ comparisons are not shown here since no single set of plots could contain all configurations simultaneously.

Table 4.2: Throughput and Spectral Efficiency for MTMR Approaches, 4x4

$Throughput$	BF	$SelTX$	$STBC$	$Psiso$
$bps/(sub-streams \times Hz)$	bps/Hz	bps/Hz	bps/Hz	bps/Hz
0.33	0.33	0.33	0.44	0.08
0.5	0.5	0.5	0.67	0.125
0.67	0.67	0.67	0.89	0.17
1	1	1	1.33	0.25
1.33	1.33	1.33	1.78	0.33
1.5	1.5	1.5	2	0.38
2	2	2	**2.67**	**0.5**
2.25	2.25	2.25	3	0.56
2.67	**2.67**	**2.67**	3.56	**0.67**
3	3	3	4	0.75
4	4	4	5.33	1
4.5	4.5	4.5	6	1.13
6	6	6	8	1.5

4.3 Scheduler Approaches

In the single-band case, the frequency band can be chosen to simply maximize SNR, but for the multi-band approach, the problem is much more difficult. Even for a small number of transmit and receive antennas, and unoccupied frequencies, there are a huge number of possible ways to assign these resources, and thus a scheduler must be designed to perform this task.

Before discussing scheduler approaches, we note that the solution space consists of an array whose dimensions are defined by the number of transmitting and receiving elements

(or sources and sinks) and by the number of unoccupied or unassigned channels. These variables are labeled N_t, N_r and N_c respectively. A single assignment consists of a transmitter, a receiver and an available channel and a complete solution consists of N_t simultaneous assignments within the solution space. Since no sources may share channels, they also may not share sinks and thus a complete solution may be visualized as a set of N_t disjoint elements in the solution space array. Obviously, the number of potential sinks and available channels are lower bounded as $N_t \leq N_r$ and $N_t \leq N_c$, and potentially the final solution may consist of fewer assignments within a solution than there are sources, but for this work, it is assumed that every source is assigned in every solution.

Because each assignment utilizes a different frequency, the assumption is made that each assignment is also interference-free from the other assignments within a solution. Without interference, the assignments are merely associated with the appropriated channel gain for a particular grouping of transmitter, receiver and unoccupied frequency band and their individual performance is determined by the absolute value of those complex-valued gains. Finally, transmitter powers are assumed to be equal for each source, the noise powers are equal for each sink.

Now that the solution space is defined, the two main approaches evaluated for finding solutions to the problem of multi-channel, multi-antenna resource allocation can be considered. The first goal of the scheduler for the proposed multi-band technique is that the solution should maximize energy efficiency. That is, assuming the signaling scheme is equivalent across all assignments within a solution, the average Symbol Error Rate (SER) and

Bit Error Rate (BER) must be minimized. The second goal for the scheduler is that it be computationally efficient and it's complexity must not increase too quickly as the solution space gets larger. That is, as N_t, N_r and/or N_c increase, the time to find the solution should increase as slowly as possible. As will be shown, achieving either of these goals is not difficult, but achieving them simultaneously presents a challenge.

The first approach, which is called $max - max$, is an iterative assignment method which seeks to maximize the channel gain for each subsequent assignment until a solution is completed. On the first iteration, the maximum channel gain is chosen and the associated source, sink and channel are synchronized to the same frequency and the remaining assignments that are associated with those resources are stricken from the solution space. In subsequent iterations, the maximum gain is chosen from the surviving elements and its associated resources are assigned and removed from further iterations in the same manner. This process continues until all the sources or transmitting elements are assigned and the solution is complete. Although this method results in the first assignment having an excellent channel with high probability, subsequent assignments are impacted by the reduction in available assignments until the final assignment is made. For small solution spaces, this method results in a solution where the final assignment made has a very high probability of using a very poor channel. For systems where $N_r >> N_t$ and/or $N_c >> N_t$ the effect is less severe. However, when $N_r = N_t$ and $N_c = N_t$, there exists only one possible assignment on the last iteration, thus maximizing the probability of a poor channel for at least one assignment within the solution.

The benefit of the $max - max$ based scheduler is its simplicity. The algorithm, while operating on a reduced number of assignments on each iteration, must only find the maximum gain element within the solution space each time and the number of iterations is equal to the number of sources or transmitters that must be assigned. Thus it meets the goal for minimizing the time to solution. The goal of maximizing energy efficiency, however, is not met since the SER and BER performance will be dominated by the poorest performing assignment in the solution and with at least one poor channel assignment, the overall performance will be severely degraded. While increasing the number of receivers or available channels sufficiently may counteract this concern, it can not be guaranteed that radio and/or network resources will always be greater than the minimum number required.

The second approach, which is called $max-min$ is also iterative, but it considers complete solutions and seeks to maximize, from smallest to largest, the gains for each assignment within a solution. While a new and reduced complexity implementation will be discussed in 4.8, as originally implemented, the first iteration of the $max - min$ scheduler assembles a complete solution consisting of N_t assignments. The first solution merely consists of the the first transmitter and receiver being assigned to the first available band, the second transmitter-receiver pair on the second available band and so on with each assignment disjoint from the others. On each subsequent iteration, the scheduler finds the next permutation of the solution by changing a single assignment and compares the resulting solution to the existing one. If the subsequent solution improves any of the assignment gains without decreasing any of the smaller gains within the solution, the potential solution is updated

with the current one. If, however, none of the assignment gains are improved, at least one gain is improved but a smaller gain is further decreased, or no gains are improved and at least one is decreased, the current solution is discarded and the scheduler moves on to the next permutation and this continues until all possible solutions are exhaustively evaluated. The resulting solution will consist of a set of N_t assignments where no assignment can be improved without decreasing a lower order assignment gain within the solution.

In Figure 4.1, below, the $max-max$ and $max-min$ schedulers are compared by showing the distributions of the gains for each assigned sub-stream. As can be seen, the while the maximum gains achieved by the $max - min$ scheduler are not as high as those for the $max-max$ scheduler, the weighting of the distribution for the worst gain is far better. This effect is mitigated as the number of available channels, N_c is increased further, while the disparity is magnified as spatial correlation is decreased. Since it is the distribution of the worst gain which will ultimately dominate performance, this gives a visual demonstration of the importance of the $max - min$ scheduler for a multi-antenna, multi-band system using transmitters with equal power and all using the same constellation size.

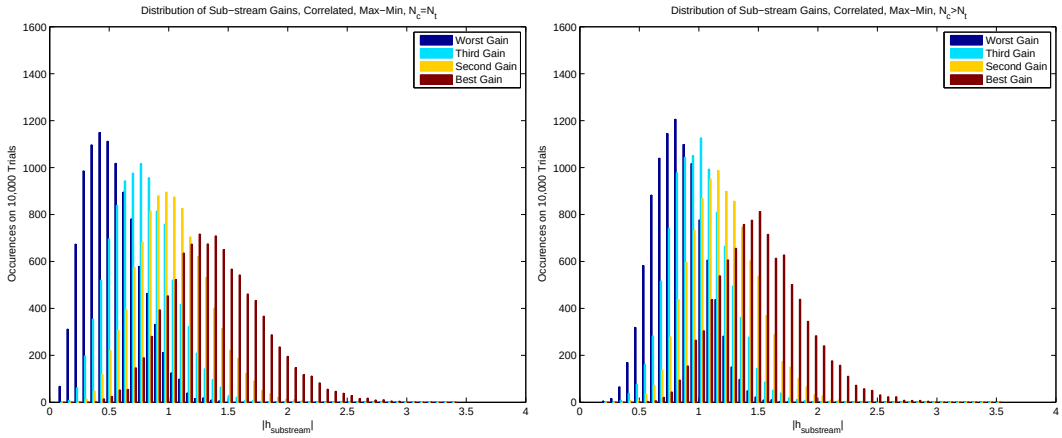

(a) $max - min$, $N_c = N_t$, High Correlation (b) $max - min$, $N_c > N_t$, High Correlation

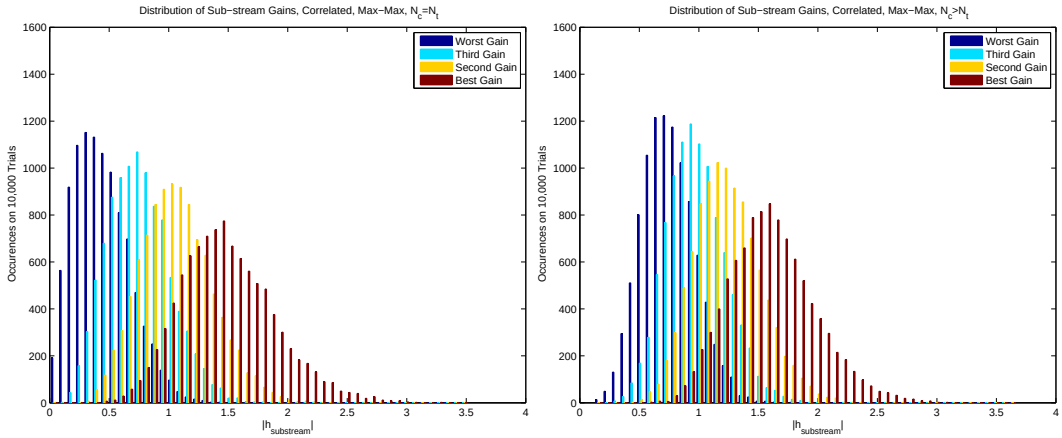

(c) $max - max$, $N_c = N_t$, High Correlation (d) $max - max$, $N_c > N_t$, High Correlation

Figure 4.1: Distributions of Sub-stream Gains for Max-Min and Max-Max, Correlated

In Figure 4.2, below, the spatial correlation is removed and the effect is even more dramatic, compounding the importance of the appropriate scheduling.

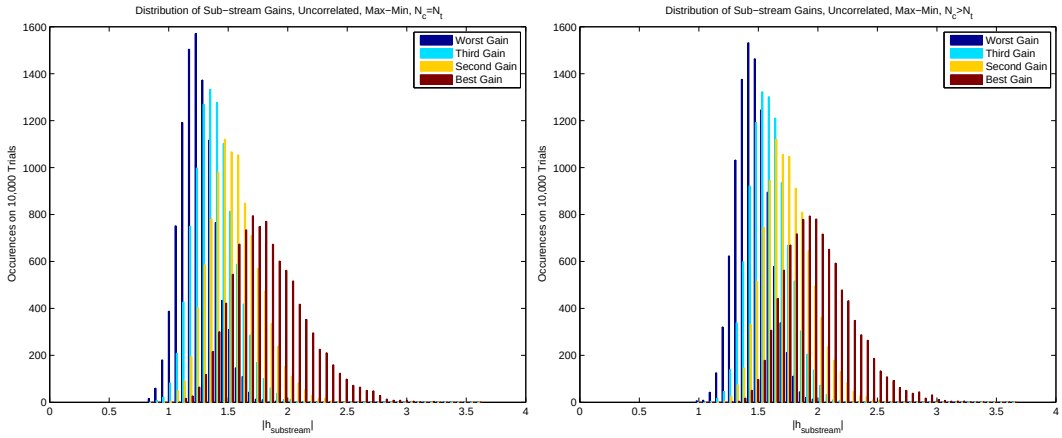

(a) $max - min$, $N_c = N_t$, Low Correlation (b) $max - min$, $N_c > N_t$, Low Correlation

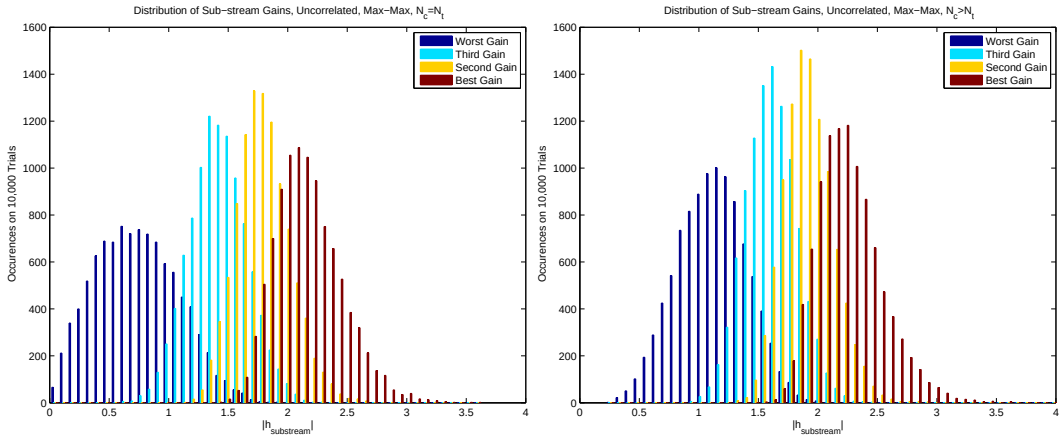

(c) $max - max$, $N_c = N_t$, Low Correlation (d) $max - max$, $N_c > N_t$, Low Correlation

Figure 4.2: Distributions of Sub-stream Gains for Max-Min and Max-Max, Uncorrelated

The benefit of the $max - min$ based scheduler is the guaranteed optimal energy efficient solution for uncoded transmission with equal-power and equal constellations on each transmit antenna. This method minimizes the BER, from worst to best, of each assign-

ment, thus eliminating the concern of one assignment's performance dominating the overall performance. While the best assignment in a $max - min$ solution will likely have poorer gain and performance than the best (first) assignment made in the $max - max$ scheduler, it still contributes far fewer errors than the worst assignment and thus does little to limit the average error performance of the overall solution.

While the energy efficiency goal is met by the $max - min$ scheduler, the penalty for such performance is paid in its complexity. The number of solutions grows very quickly with increasing dimensionality of the solution space and thus the number of solutions this scheduler must evaluate (and subsequently, the time to solution) grows at an equal rate. Since guaranteed optimal performance is desired, it is not desirable to eliminate evaluating available channels or receivers, or limit the number of transmitters in the global solution. However, since the dimensionality of the solution space can not be limited, an acceptable time to solution with increasing radio and network resources can not be guaranteed. To illuminate the complexity issue for the $max - min$ scheduler, the number of solutions in terms of the solution space dimensions is defined in Equation 4.1where N_s is the number of potential solutions and a few data points are listed in Table 4.3 for relatively small solution spaces.

$$N_s = \prod_{i=0}^{N_t-1} (N_r - i)(N_c - i)) \tag{4.1}$$

The performance of $max - max$ and $max - min$ schedulers for an $N_t = 2$, $N_r = 2$ system are compared as the number of available channels is increased, $N_c = 2, 4, 8$ in Figures 4.3,4.4

Table 4.3: Solutions for Small Spaces

$N_c \diagdown N_t \times N_r$	2×2	4×4
2	4	-
3	12	-
4	24	576
5	40	2880
6	60	8640
7	84	20160
8	112	40320

and 4.5, respectively. For this comparison, uncoded QPSK is used. For all solution space realizations for this work, the available channels are are assumed to be i.i.d with no spectral correlation.

As can be seen, the $max - min$ scheduler is always superior to the $max - max$ scheduler. For both schedulers, performance improves with the availability of additional channels. More importantly, when available channel resources are limited, the difference in performance between the two schedulers is substantial. From this point on, a scheduler using the $max - min$ criteria is used for the multi-channel transmit diversity system called Parallel SISO.

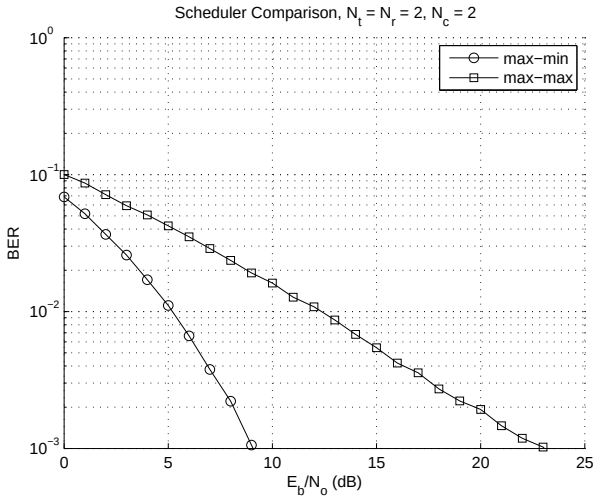

Figure 4.3: Scheduler Performance Comparison, 2 Channels

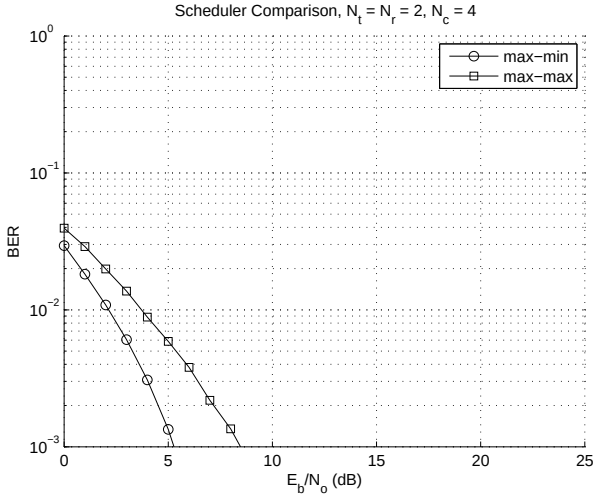

Figure 4.4: Scheduler Performance Comparison, 4 Channels

4.4 Performance of Transmit Diversity Schemes

First, the performance of the four systems will be shown. For comparison, the equal power transmit diversity scheme that can be compared directly to Parallel SISO is STBC. Performance for beamforming and transmit selection diversity schemes will be compared as

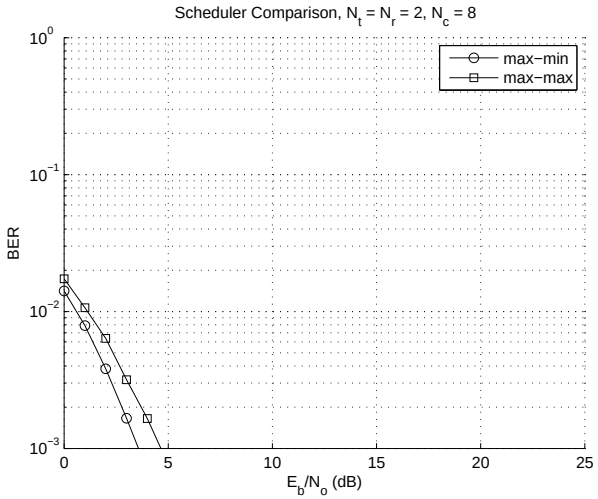

Figure 4.5: Scheduler Performance Comparison, 8 Channels

well, with the caveat that they require additional PA flexibility and feedback information. Since a single-channel DSA was used for each of the single-channel, MIMO-based diversity schemes, their performances with respect to spatial correlation and rate of improvement with increasing number of available channels will also be of interest.

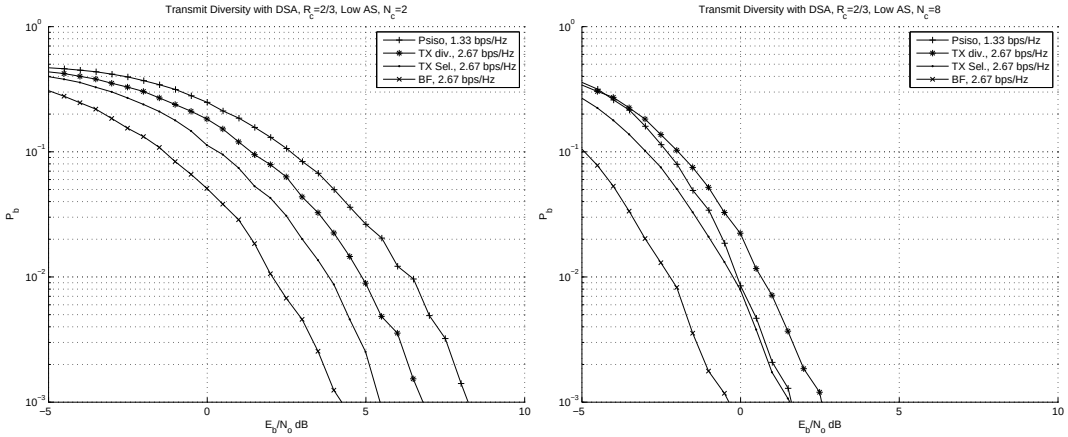

(a) 2 Bands, High Correlation

(b) 8 Bands, High Correlation

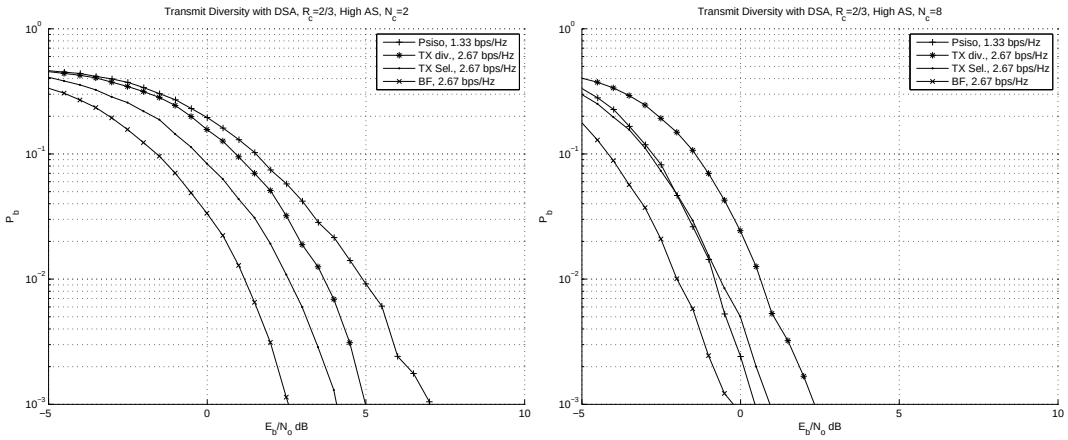

(c) 2 Bands, Low Correlation (d) 8 Bands, Low Correlation

Figure 4.6: Multi- and Single-Channel DSA, 2x2, Coded

With a small number of channels and high spatial correlation (ρ), the results are exactly what would be expected. Beamforming, which requires CSIT and a flexible PA, outperforms the other schemes, followed by transmitter selection, STBC and finally Parallel SISO. Moving to a larger number of open channels with high correlation however, shows that Parallel SISO outperforms STBC by about 1 dB E_b/N_o. With a higher number of available channels and low spatial correlation, Parallel SISO not only outperforms STBC by about 2 dB E_b/N_o, but it is also beginning to outperform transmitter selection.

Given these results, it becomes desirable to have a system which automatically chooses the scheme which for a given channel, achieves the best energy efficiency. The metrics which make such decision-making possible are developed in the next section.

4.5 Developing Metrics For Adaptation

With the use of channel coding, it is desirable to know the exact gain and hence, distance properties of the codes being used. As the $R_c d_{free}$ metric, or channel code rate multiplied by it's minimum free Hamming distance, provides the means to determine the asymptotic performance gain, it is implicit that this gain is only realized at arbitrarily low bit error rates and does not account for the weight spectrum of the code being used. Since the systems being evaluated are intended to operate around $P_b = 10^{-3}$, Monte-Carlo simulations were used to determine the equivalent $R_c d_{free}(BER = 10^{-3})$ or distance metric for the codes being used. Where $R_c d_{free}$ indicates the asymptotic performance gain, the equivalent $R_c d_{free}(BER = 10^{-3})$ is determined in order to find $d_{comp,code}$, or the compensation factor for the channel code. In Table 4.4, these realizable metrics are shown and the metric, $d_{comp,code}$ is introduced to convey the difference between the asymptotic gain and the gain seen at the operating point. Together, $R_c d_{free} d_{comp,code}$ reflects the actual performance gain from the channel code being used at the BER of interest.

To predict performance of the various schemes, the familiar equations for BER approximation are modified to account for the diversity gains commensurate with each system and to account for channel coding. The modified equations take the form below, with special care given to keep terms separate to enable their use in the adaptive algorithms that will be developed. In these equation, d_{min} is the minimum Euclidean distance based on a normalized average signal power as shown in Table 2.1.

Table 4.4: FEC Free Distance Compensation

R_c	d_{free}	$R_c d_{free}$	$R_c d_{free}(BER = 10^{-3})$	$d_{comp,code}$
$\frac{3}{4}$	6	4.5	2	0.45
$\frac{2}{3}$	7	4.7	2.28	0.485
$\frac{1}{2}$	10	5	2.7	0.54
$\frac{1}{3}$	16	5.3	3	0.57
$\frac{1}{4}$	22	5.5	3.1	0.56
$\frac{1}{6}$	34	5.7	3.2	0.56

$$P_{b,QPSK} = Q\left(\sqrt{d_{MIMO}\frac{d_{min}^2}{2}R_c d_{free} d_{comp,code}\frac{E_b}{N_o}}\right) \tag{4.2}$$

$$P_{b,8-PSK} \approx \frac{1}{\log_2(M)} 2Q\left(\sqrt{d_{MIMO}\frac{d_{min}^2}{2}R_c d_{free} d_{comp,code}\frac{\log_2(M)E_b}{N_o}}\right) \tag{4.3}$$

$$P_{b,16-QAM} \approx \tag{4.4}$$
$$\frac{1}{\log_2(M)}\frac{1}{4}2Q\left(\sqrt{d_{MIMO}\frac{d_{min}^2}{2}R_c d_{free} d_{comp,code}\frac{\log_2(M)E_b}{N_o}}\right) +$$
$$\frac{1}{\log_2(M)}\frac{1}{2}3Q\left(\sqrt{d_{MIMO}\frac{d_{min}^2}{2}R_c d_{free} d_{comp,code}\frac{\log_2(M)E_b}{N_o}}\right) +$$
$$\frac{1}{\log_2(M)}\frac{1}{4}4Q\left(\sqrt{d_{MIMO}\frac{d_{min}^2}{2}R_c d_{free} d_{comp,code}\frac{\log_2(M)E_b}{N_o}}\right)$$

$$P_{b,64-QAM} \approx \tag{4.5}$$
$$\frac{1}{\log_2(M)}\frac{1}{16}2Q\left(\sqrt{d_{MIMO}\frac{d_{min}^2}{2}R_c d_{free} d_{comp,code}\frac{\log_2(M)E_b}{N_o}}\right) +$$
$$\frac{1}{\log_2(M)}\frac{3}{8}3Q\left(\sqrt{d_{MIMO}\frac{d_{min}^2}{2}R_c d_{free} d_{comp,code}\frac{\log_2(M)E_b}{N_o}}\right) +$$
$$\frac{1}{\log_2(M)}\frac{9}{16}4Q\left(\sqrt{d_{MIMO}\frac{d_{min}^2}{2}R_c d_{free} d_{comp,code}\frac{\log_2(M)E_b}{N_o}}\right)$$

The newly introduced distance and gain terms are defined for each of the transmit diversity systems below.

$$d_{MIMO,STBC} = \sum_{j=0}^{N_t-1}\sum_{i=0}^{N_r-1}\frac{|h_{i,j}|^2}{N_t N_r} \tag{4.6}$$

In Equation 4.7 below, σ_n are the singular values resulting from the decomposition of the MIMO channel matrix and λ_{max} corresponds to the maximum singular value.

$$d_{MIMO,BF} = \frac{(\max\{diag(\sigma_1, \sigma_2, ..., \sigma_{N_t})\})^2}{N_t} = \frac{\lambda_{max}}{N_t} \tag{4.7}$$

$$d_{MIMO,TXsel} = \arg \max_{j \in 0 \ldots N_t - 1} \{ \sum_{i=0}^{N_r - 1} \frac{|h_{i,j}|^2}{N_r} \} \tag{4.8}$$

$$d_{MIMO,Psiso,uncodedand2or3TXcoded} = \min\{|h_{i_1,j_1,k_1}|^2 \ldots |h_{i_{N_t},j_{N_t},k_{N_t}}|^2\} \tag{4.9}$$

$$d_{MIMO,Psiso,4TXorgreater,coded} = mean\{|h_{i_1,j_1,k_1}|^2 \ldots |h_{i_{N_t},j_{N_t},k_{N_t}}|^2\} \tag{4.10}$$

Here, $\{|h_{i_1,j_1,k_1}| \ldots |h_{i_{N_t},j_{N_t},k_{N_t}}|\}$ is the list of gains returned by the max-min scheduler.

As can be seen, two different distance metrics must be defined for Parallel SISO. For uncoded Parallel SISO or coded systems with fewer than 4 transmit antennas, the minimum gain will dominate performance and thus the pessimistic BER estimate will be based on the worst performing sub-stream. For Parallel SISO using coding and interleaving across the sub-streams and with at least 4 transmit antennas, the mean of the squares of the channel gains reflects the average of the SNRs on each of the sub-streams. This relationship was predicted by examining the distribution of the gains returned by the $max - min$ which revealed small disparity between the maximum and minimum gains with larger arrays, in combination with the use of Side Information (SI), or channel gains experienced by the symbols and their respective bits, in the demodulator to produce the LLRs being fed into the Viterbi decoder.

4.6 Distance Metric-based Adaptation

In order to develop metrics that are attractive for implementation, and which do not rely on calculation of actual BER at run-time, the desired BER for operation is defined beforehand to determine the argument under the radical in the Q function for each of the BER equations shown earlier. Setting a desirable BER of 10^{-3}, the BER equations are solved to find this argument for each of the constellations to be used. In Table 4.5 below, the arguments under the radical required to achieve the goal BER for each constellation are listed. For convenience, this will be called d_{req}, or the required overall distance for the particular multi-antenna scheme, constellation, code rate and $\frac{E_b}{N_o}$.

Table 4.5: Distances Required For Desired BER

$Constellation$	$d_{required}\ for\ P_b = 10^{-3}$
$QPSK$	9.54
$8-PSK$	8.81
$16-QAM$	9.02
$64-QAM$	8.56

Now, terms are combined and the equations are simplified to make them in terms of SNR rather than $\frac{E_b}{N_o}$ and will reflect the actualized distance. Using $SNR = d_{MIMO}\frac{\log_2(M)E_b}{N_o}$, the

actual distance, d_{actual} is expressed below in 4.11.

$$d_{actual} = R_c d_{free} d_{comp,code} \frac{d_{min}^2}{2} SNR \tag{4.11}$$

Next, a decision statistic is defined to express the relative performance expected from each potential multi-antenna scheme.

$$z_{MIMO} = \frac{d_{actual}}{d_{required}} \tag{4.12}$$

The expected performance can be determined from a single statistic for each multi-antenna scheme. When $z_{MIMO} < 1$, the expected BER will not meet the desired constraint, but when $z_{MIMO} \geq 1$, the particular multi-antenna scheme, with its respective code rate and constellation can be expected to perform as desired.

Finally, since the main goal of this work is to choose the most robust scheme, it can be chosen on the basis of $\max\{z_{MIMO,1} \ldots z_{MIMO,n}\}$. When CSIT is not available and there is no transmitter specific feedback, the decision would be made based on choosing between STBC and Parallel SISO as in Equation 4.13.

$$z_{MIMO,adaptive} = \max\{z_{MIMO,STBC}, z_{MIMO,Psiso}\} \tag{4.13}$$

When the equal power constraint is removed and the feedback channel is augmented to provide transmit antenna selection, the choice is made according to Equation 4.14.

$$z_{MIMO,adaptive} = \max\{z_{MIMO,STBC}, z_{MIMO,Psiso}, z_{MIMO,TXsel}\} \tag{4.14}$$

Finally, when there is no restriction on power allocation at the transmitter and full CSIT is assumed, the decision is made according to Equation 4.15.

$$z_{MIMO,adaptive} = \max\{z_{MIMO,STBC}, z_{MIMO,Psiso}, z_{MIMO,TXsel}, z_{MIMO,BF}\} \tag{4.15}$$

Using the metrics shown above an adaptation algorithm can be made to choose, using SNR and the constellation and code rate distances, the scheme which will yield the smaller BER.

In Figure 4.7, both the original systems and three new adaptive curves are shown on each plot according to the metrics that have been established. From the plots, the adaptive system limited to equal power for each element, without explicit information about the channel or the number of available bands and without computing BER at run time, is able to choose the best scheme on a channel and SNR basis. Although it is not a fair comparison, the adaptive systems which are allowed to consider transmit selection and beamforming as well are able to choose correctly. In the case of beamforming though, there is not much to choose from since beamforming is generally so much better performing than the other schemes. In the channel with only two bands and high spatial correlation, the equal power adaptive system actually outperforms both the systems from which it chooses because when the schemes being considered are close enough, the left hand tail of the poorer performer weights the overall distribution towards lower required E_b/N_o. In the case where there are many more open frequency bands than required, the adaptive system which considers the equal power schemes plus the transmit selection actually outperforms those three schemes because of the

overlapping distributions. Only in the case with low spatial correlation and a greater number of available frequencies does the equal power adaptive system perform a fraction of a decibel worse than the best scheme, due to the pessimistic BER metric for transmit arrays using coding with fewer antennas.

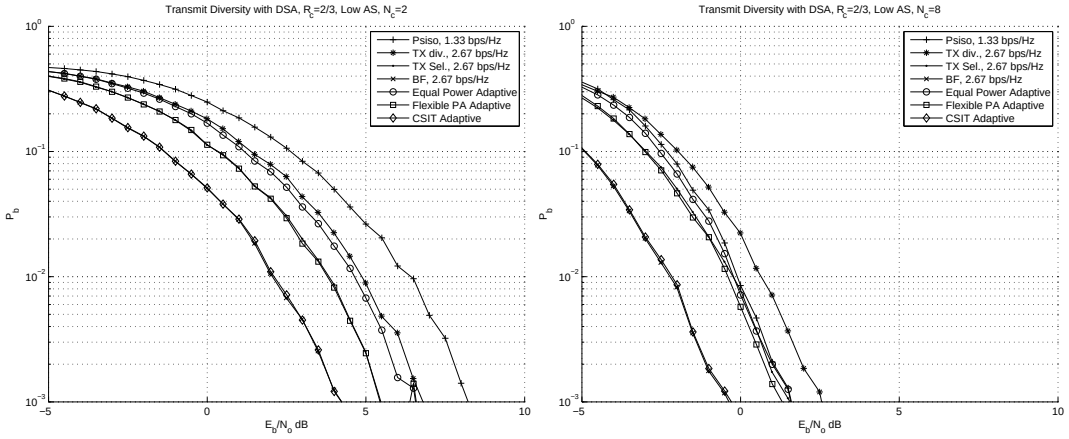

(a) 2 Bands, High Correlation

(b) 8 Bands, High Correlation

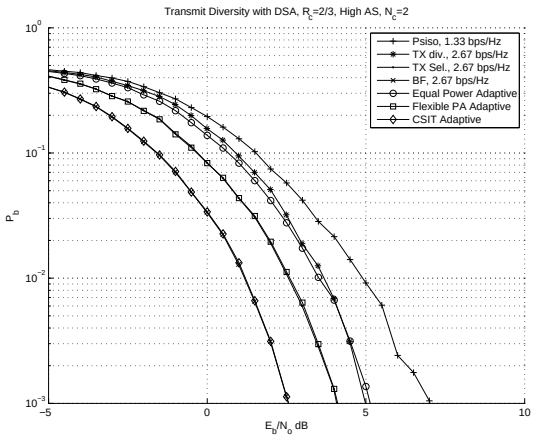

(c) 2 Bands, Low Correlation

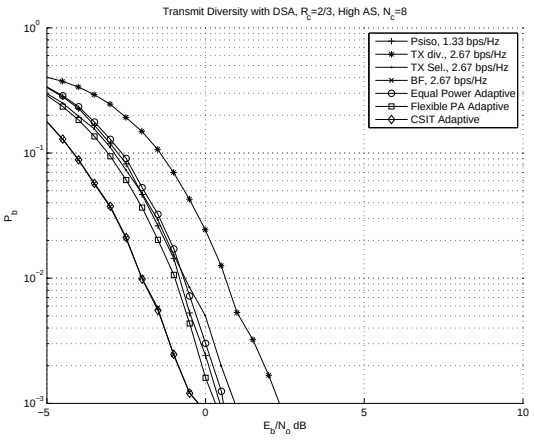

(d) 8 Bands, Low Correlation

Figure 4.7: Multi- and Single-Channel DSA and Adaptation, 2x2, Coded

4.7 Trends with Larger Arrays

When considering energy efficient configurations for multi-antenna systems with more antennas, there are several trends to consider. For single-channel systems, the diversity gains decrease with each additional diversity branch, and for the same system, the Parallel SISO system is permitted to use additional channels, requiring constellations with fewer and fewer points to maintain a constant throughput. Also, as the parallel SISO system is allowed to use smaller constellations, it is operating closer to the region of the channel capacity curve where incremental increases in SNR yield greater increases in capacity. Finally, in the case of equal power transmit diversity systems, as mentioned in Chapter 2, as the number of transmit antennas increases, the code rate for STBCs decreases from $R = 1$ for 2 transmit antennas, to $R = \frac{3}{4}$ for 3 and 4 transmit antennas, and finally to $R = \frac{1}{2}$ for 5 or more transmit antenna. The decreasing rate of STBCs with number of transmit antennas further compounds the required spectral efficiency of a single-band system to equal the throughput of a multi-channel configuration of the same system. These factors considered, the bandwidth expansion factor of the parallel SISO system allows it to increase the margin of performance over the single-channel equivalent. This is of course, an intuitive result, as bandwidth expansion is expected to yield improvements in energy efficiency. The key to making this trend possible for for multi-channel, multi-antenna resources, is the scheduler used to allocate resources.

4.8 Fast Implementation of the $max - min$ Scheduler

Having finished the discussion of energy efficient configuration of multi-antenna systems and having established the importance of the $max - min$ scheduler for multi-band energy efficiency, a more computationally efficient implementation that was developed to address the potential problems with the time to solution will be discussed. Ideally, increases in time to solution would be linear with the increases in sources, sinks and available channels, and it was quickly established that any attempt to streamline the process would have to yield the exact same solutions as the original implementation of the $max - min$ scheduler but would have to search the solution space without evaluating each solution.

Since the main goal of the $max - min$ scheduler is to eliminate the poorest gains from the final solution, the approach taken was to iteratively find the minimum gains, and puncture them from the solution space one by one. At each iteration, the new scheduler evaluates the surviving elements in the solution space to make sure that a solution is still possible once the puncture is made. If the puncture is not possible, the element remains and the scheduler resumes by evaluating the next smallest gain in the solution space. The scheduler continues this process until each gain is evaluated and punctured or left alone. By this process, the scheduler only evaluates N_t by N_r by N_c elements. The punctured solution space is guaranteed to have at least one solution, but more importantly, contains a vastly reduced number of solutions which are now evaluated according to the max-min criteria. This non-linear approach results in the same final solution as the scheduler that evaluates the non-punctured solution space. The original and improved implementations were presented with $10,000$

spatially uncorrelated and $10,000$ spatially correlated channels and their ordered gains were compared numerically to assure equivalence. In Figure 4.8, below, the ordered gains from the exhaustive implementation were plotted on the y-axis against the ordered gains from each channel realization of the fast implementation on the x-axis. The $slope = 1, intercept = 0$ lines demonstrate visually the equivalence in solutions between the exhaustive and efficient implementations under varying spatial correlation and available channels.

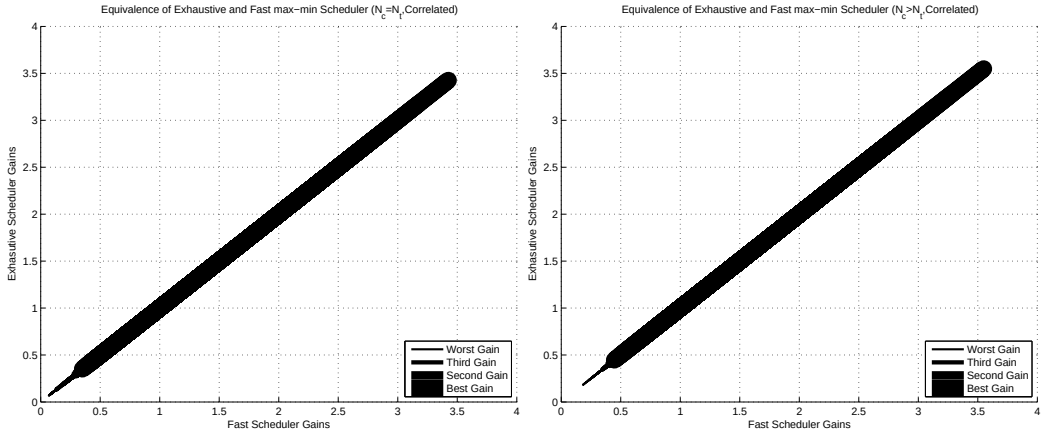

(a) $N_c = N_t$, High Correlation

(b) $N_c > N_t$, High Correlation

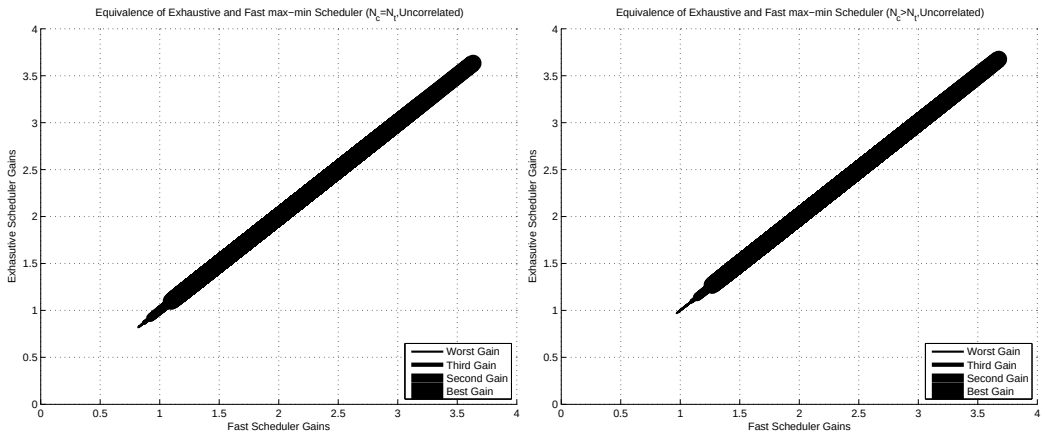

(c) $N_c = N_t$, Low Correlation (d) $N_c > N_t$, Low Correlation

Figure 4.8: Equivalence of Exhaustive and Fast $max - min$ Scheduler Solutions

To demonstrate the efficiency of the new implementation, the scheduler was run for 10,000 realizations of a $N_t = 4$, $N_r = 4$ system, with $N_c = 4, 6, 8$. From Equation 4.1 and Table 4.3, the original $max - min$ scheduler must evaluate 576, 8,640 and 40,320 solutions for those same solution spaces.

As can be seen in Figure 4.9, this non-linear approach results in a distribution for the number of solutions that must be evaluated at the conclusion of the puncturing process. For the spaces shown here, not one trial resulted in more that 50 solutions requiring evaluation by the scheduler with most trials resulting in fewer that 10.

It was also desirable to consider the effect of spatial correlation between antennas, so the antennas of the transmitters and receivers were modeled as part of a linear array in a multi-path channel with very little angle spread, resulting in high correlation between the antenna elements. The same trials were performed with the solution space reflecting this

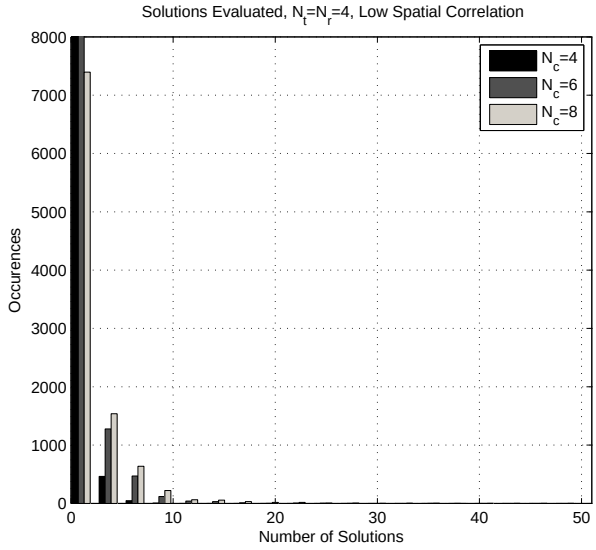

Figure 4.9: Distribution of Remaining Solutions After Puncturing, Low Spatial Correlation

high level of spatial correlation while leaving the available channels uncorrelated. The results are shown below in Figure 4.10.

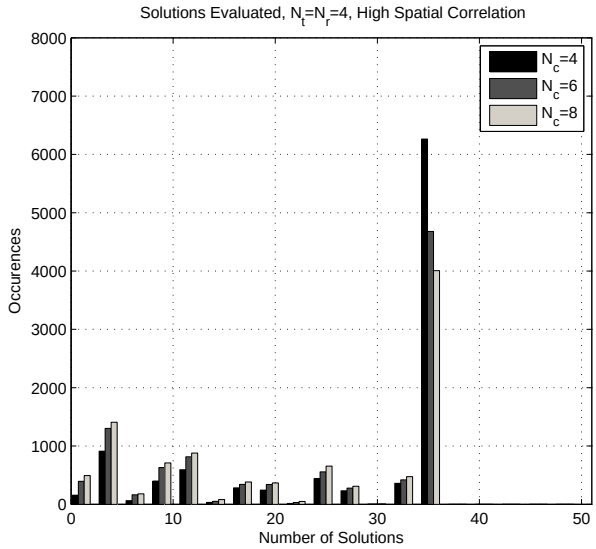

Figure 4.10: Distribution of Remaining Solutions After Puncturing, High Spatial Correlation

Again, the drastic reduction in complexity with the efficient implementation of the $max-min$ scheduler is evident. Though the distribution has changed, no trial resulted in greater than 40 solutions requiring evaluation. The change in distribution is caused by the correlation since elements the puncturing tends to focus on the channels where correlated elements are all affected by small gains, thus leaving other channels that are barely punctured and leaving a greater number of solutions including elements from the better channels.

To further demonstrate the improvement, and using Matlab implementations, the time to solution was evaluated and averaged over a large number of channel realization for both the original $max-min$ method and the computationally efficient implementation while varying the size of the search space. The following plots compare the time to solution for the two implementations with $N_f = 4$ and $N_f = 8$ under low spatial correlation.

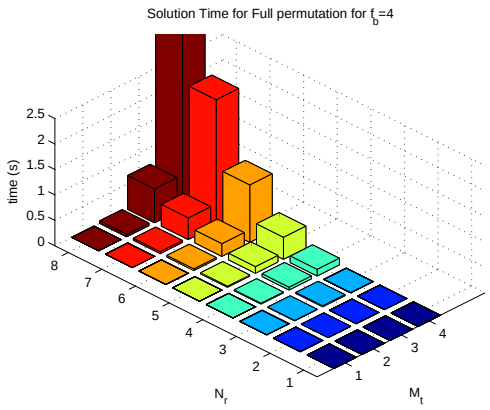

(a) Original, 4 Unoccupied bands

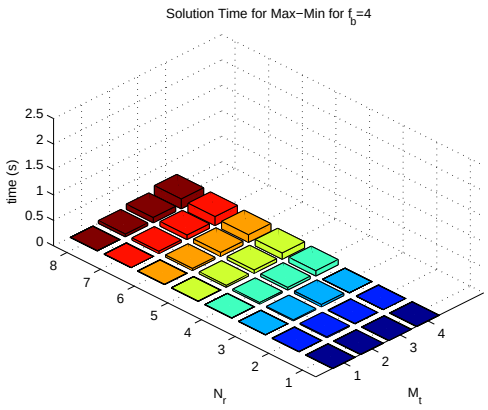

(b) Efficient, 4 Unoccupied bands

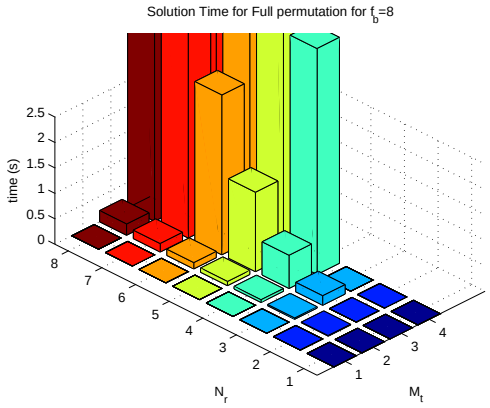

(c) Original, 8 Unoccupied bands

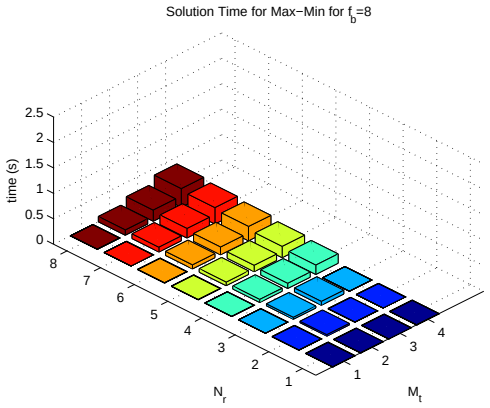

(d) Efficient, 8 Unoccupied bands

Figure 4.11: Comparison of Original and Computationally Efficient max-min Schedulers for Multi-Band Links

4.9 Robust Multi-Antenna Adaptation Conclusions

In this chapter, MTMR systems were examined in the context of their ability to achieve high levels of energy efficiency. Assuming a fixed throughput requirement, and taking into consideration CSIT availability and PA configurability, one novel multi-band and three single-band configurations were examined and characterized. Metrics were developed to predict the performance of each configuration and a method for automatic adaptive reconfiguration using these metrics and based on channel and network parameters was described. The metrics and adaptive algorithm were shown to be able to take CSIT and PA parameters into account, evaluate the metrics for the appropriate configurations and choose the best MTMR scheme which maximized energy efficiency. When the difference in performance between the avail-

able schemes was small enough, the adaptive algorithm was able to achieve better average performance than the individual schemes alone.

Chapter 5

Spectral Efficiency

To approach the problem of maximizing spectral efficiency of a MIMO system, additional metrics must be defined for the remainder of the MIMO configurations which are to be considered. While in Chapter 4, we considered diversity-only schemes and assumed that the SNR was too low to support spatial multiplexing, we now assume that the SNR varies over a wide enough range that spatial multiplexing scheme can be supported when spatial correlation becomes sufficiently small and SNR becomes sufficiently high. Specifically, the performance of spatial multiplexing schemes must be characterized as a function of system and channel parameters and developed into metrics which will allow the automatic selection of a MIMO scheme that will maximize spectral efficiency while meeting a BER a constraint. The adaptive systems will now consider only single-band MIMO schemes including both diversity and spatial multiplexing modes.

5.1 MoDem-CoDec Codebook Creation

First, because this level of adaptation will require the joint configuration of MoDem, CoDec and MIMO scheme, it will greatly simplify things to create the MoDem-CoDec configuration codebook first. The normalized minimum Euclidean distances and the distance metrics for the channel codes are used to generate the list of joint MoDem/CoDec configurations. Using the spectral efficiency and distance metrics for each combination of constellation and code rate, a list was generated and pruned so that for a decrease in spectral efficiency from one combination to the next, it is accompanied by a corresponding increase in energy efficiency. With QPSK, 8-PSK, 16-QAM and 64-QAM and convolutional codes with rates between $\frac{3}{4}$ and $\frac{1}{6}$ and their respective distances given by Tables 4.4 and 4.5, the unpruned list would potentially yield 28 combinations of MoDem and CoDec, many of which have overlapping spectral efficiencies. In Table 5.1 below, the possible spectral efficiencies for all possible combinations of MoDem and CoDec are shown before pruning. The pruned list contains only 13 total combinations which are guaranteed to effectively 'surf' the spectral efficiency-energy efficiency trade off.

Taking into consideration the code distance compensation factors $d_{comp,code}$ from Table 4.4, the required distances to achieve the desired BER for each constellation in Table 4.5, the constellation and code distances from Tables 2.1 and 2.2, respectively, and finally the spectral efficiencies from Table 5.1 above, the pruned list is generated as described above and shown in Table 5.2 below.

Beginning with the framework which was developed earlier, the metrics and adaptive

Table 5.1: Spectral Efficiency For MoDem-CoDec Combinations

$CoDec \diagdown MoDem$	$QPSK$	$8-PSK$	$16-QAM$	$64-QAM$
$\frac{1}{6}$	0.33	0.5	0.67	1
$\frac{1}{4}$	0.5	0.75	1	1.5
$\frac{1}{3}$	0.67	1	1.33	2
$\frac{1}{2}$	1	1.5	2	3
$\frac{2}{3}$	1.33	2	2.67	4
$\frac{3}{4}$	1.5	2.25	3	4.5
$Uncoded$	2	3	4	6

process will be a modified version of these metrics. For maximization of spectral efficiency, the single-band diversity schemes will be used in addition to the spatial multiplexing schemes which will be developed here. Again, the MIMO distance metrics for these single-band diversity approaches are listed in Equations 5.1, 5.2 and 5.3.

$$d_{MIMO,STBC} = \sum_{j=0}^{N_t-1} \sum_{i=0}^{N_r-1} \frac{|h_{i,j}|^2}{N_t N_r} \tag{5.1}$$

$$d_{MIMO,BF} = \frac{(\max\{diag(\sigma_1, \sigma_2, ..., \sigma_{N_t})\})^2}{N_t} = \frac{\lambda_{max}}{N_t} \tag{5.2}$$

$$d_{MIMO,TXsel} = \arg \max_{j \in 0...N_t-1} \{ \sum_{i=0}^{N_r-1} \frac{|h_{i,j}|^2}{N_r} \} \tag{5.3}$$

Table 5.2: Pruned MoDem-CoDec Codebook

$MoDem-CoDecIndex$	$Constellation$	$CodeRate$	$\eta(bps/Hz)$
1	$QPSK$	$\frac{1}{6}$	0.33
2	$QPSK$	$\frac{1}{4}$	0.5
3	$QPSK$	$\frac{1}{3}$	0.67
4	$QPSK$	$\frac{1}{2}$	1
5	$QPSK$	$\frac{2}{3}$	1.33
6	$QPSK$	$\frac{3}{4}$	1.5
7	$QPSK$	$Uncoded$	2
8	$8-PSK$	$\frac{3}{4}$	2.25
9	$16-QAM$	$\frac{2}{3}$	2.67
10	$16-QAM$	$\frac{3}{4}$	3
11	$16-QAM$	$Uncoded$	4
12	$64-QAM$	$\frac{3}{4}$	4.5
13	$64-QAM$	$Uncoded$	6

Predicting the performance for a multiplexing system is more difficult than for a diversity system because the distribution of the eigenvalues for a given MIMO channel realization is not constant, the smallest eigenmode typically dominates performance and in the case of BLAST-type systems, interference between the sub-streams makes it even more difficult to

predict the performance or interaction between the sub-streams. Since the gain metrics used for multiplexing schemes are approximations, it is more important to develop additional metrics to augment these to more closely predict performance. First, distance metrics which reflect the error dominating performance of the worst sub-stream are defined for transmit multiplexing that will be augmented by additional metrics that reflect the interaction of the multiplexing scheme with the channel coding and the channel itself.

$$d_{MIMO,BLAST} \approx \lambda_{sub-streams} \tag{5.4}$$

$$d_{MIMO,svdMUX} \approx \lambda_{sub-streams} \tag{5.5}$$

In Equations 5.4 and 5.5, it must be noted that λ_1 is the strongest eigenvalue of $HH_{\dagger}$, where *dagger* denotes the Hermitian, $sub-streams$ is the number of spatially multiplexed sub-streams transmitted resulting in the use of $\lambda_{sub-streams}$, and $1 \leq sub-streams \leq min(N_t, N_r)$. Similar to the way the distance and decision metrics were generated in Chapter 4, the actual distance, d_{actual} for spatial multiplexing schemes will require an additional term, $d_{diversity}$, with the actual distance for spatial multiplexing schemes given by Equation 5.6. The decision metric for each configuration will be generated as it was in Chapter 4 according to Equation 5.7. Since $d_{diversity}$ is only required to augment the MIMO distances for multiplexing schemes, this term is not needed when computing the MIMO distance for diversity schemes.

$$d_{actual} = d_{diversity,MUX} d_{MIMO} R_c d_{free} d_{comp,code} \frac{d_{min}^2}{2} SNR \tag{5.6}$$

$$z_{MIMO} = \frac{d_{actual}}{d_{required}} \tag{5.7}$$

The new, MIMO distance metric for the multiplexing schemes has been updated with the new term to reflect the augmentation approach that will be taken as described above. Before developing the multiplexing diversity distance augmentation, the BER constraint must once again be reflected in the definition of $d_{required}$ for each constellation to be used. Since the goal will once again be $P_b = 10^{-3}$, the values from Table 4.5 will be reused.

In the three regimes to be considered, the main factor distinguishing them is the information available at the transmitter. While the same issues with the PA configuration are still present as in Chapter 4, it is not as critical to focus on that point as it is for the difference in feedback information.

5.2 Space-Time Coding or Full Multiplexing

In the first system, or regime, the feedback channel carries only with it, the MoDem-CoDec codebook index and a bit to decide between full diversity and full multiplexing modes. For the MMSE BLAST-type multiplexing, the diversity distances, needed to first be found. Monte-Carlo simulation was that only way seen to do this. The actual, equivalent MIMO distances were found from taking the expectation of the required SNR to meet the target

BER constraint and then, the multiplexing diversity distances were found from solving for $\lambda_{sub-streams}$ which in this simple system, is just λ_{min}. It was found that this process had to be performed for each size array, each coding rate, and as a function of spatial correlation to reflect the amount of diversity available between the multiplexed sub-streams and the interaction with the channel code. In the tables, ρ is the measure of the spatial correlation between neighboring antennas at either the transmitter or receiver, for this system, assuming the transmit and receive arrays are identical.

The three tables below (5.3, 5.4 and 5.5) were then compiled for use in an adaptive algorithm based on managing the resources for the system without CSIT or transmitter-specific feedback information.

Table 5.3: Uncoded Diversity Distance, BLAST, 10^{-3}

$N_t x N_r$	$0.90 \geq \rho > 0.70$	$0.70 \geq \rho > 0.5$	$0.5 \geq \rho$
$2x2$	3	2.1	1.5
$4x4$	4	2.8	2

In Table 5.4 and all the following tables for Spatial Codeword Diversity Distances, two seemingly contradictory trends emerge. On the one hand, the distance increases with decreasing code rate, while on the other hand distance decreases with smaller values of spatial correlation. While it tends to make sense that distance would increase with decreasing code rate, the distance decreases with correlation because we are using the minimum eigenvalue

Table 5.4: Spatial Codeword Diversity Distance, 2x2, BLAST, 2 Sub-streams, 10^{-3}

R_c	$0.90 \geq \rho > 0.70$	$0.70 \geq \rho > 0.5$	$0.5 \geq \rho$
$\frac{3}{4}$	1.5	1.35	1.25
$\frac{2}{3}$	2	1.5	1.25
$\frac{1}{2}$	2	1.75	1.75
$\frac{1}{3}$	5	3.25	2
$\frac{1}{4}$	5	3.25	2
$\frac{1}{6}$	5	3.5	2

corresponding to the number of spatially-multiplexed sub-streams as a basis for the multiplexing distance. As correlation decreases, the minimum eigenvalue increases, and thus, the diversity distance for codewords decreases with the decreases in disparity between the highest and lowest eigenvalues.

In the adaptive system, the final choice of configuration will be made on the basis of z_{MIMO}. When presented with a channel realization and SNR, the adaptive algorithm computes the minimum eigenvalue as shown, chooses the appropriate diversity distance, based on array size, code rate and spatial correlation and computes d_{actual}. Then, for each of the available combinations of MoDem, CoDec and MIMO scheme, z_{MIMO} is computed. For configurations where $z_{MIMO} \geq 1$, the corresponding spectral efficiency is computed. Then, from the surviving configurations, the MoDem, CoDec and MIMO scheme are chosen to maximize

Table 5.5: Spatial Codeword Diversity Distance, 4x4, BLAST, 4 Sub-streams, 10^{-3}

R_c	$0.95 \geq \rho > 0.75$	$0.75 \geq \rho > 0.5$	$0.5 \geq \rho$
$\frac{3}{4}$	3	3	3
$\frac{2}{3}$	3	3	3
$\frac{1}{2}$	4	3.7	3.5
$\frac{1}{3}$	5	4.5	4
$\frac{1}{4}$	6.5	5.2	4
$\frac{1}{6}$	7	6.4	4

the computed spectral efficiency.

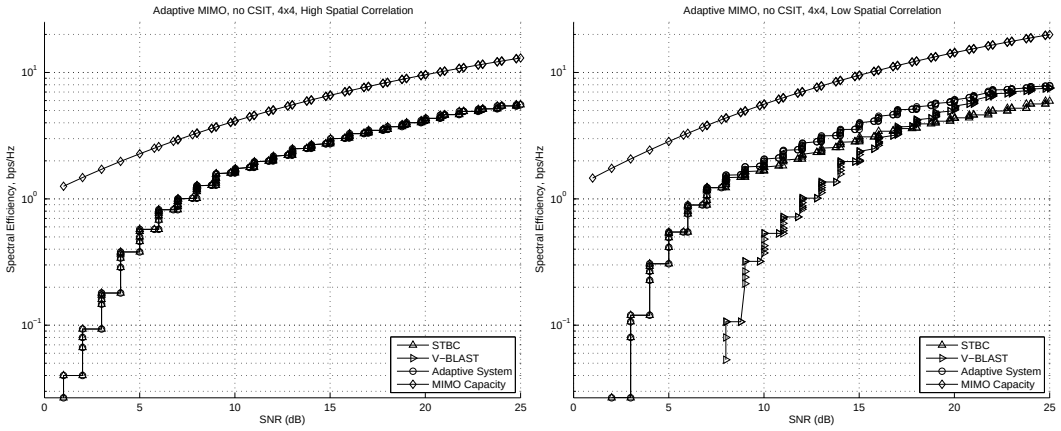

(a) High Correlation (b) Low Correlation

Figure 5.1: Performance of Adaptive MIMO without CSIT

In Figure 5.1, the capacity of the adaptive system is compared to both the channel

capacities and the full diversity and full multiplexing systems with adaptive MoDem and CoDec only. While not very interesting with high correlation, due to the channel's inability to support full multiplexing, when the channel becomes less correlated, the channel capacity increases and the adaptive system is able to capture that by 'surfing' over both diversity and multiplexing regimes.

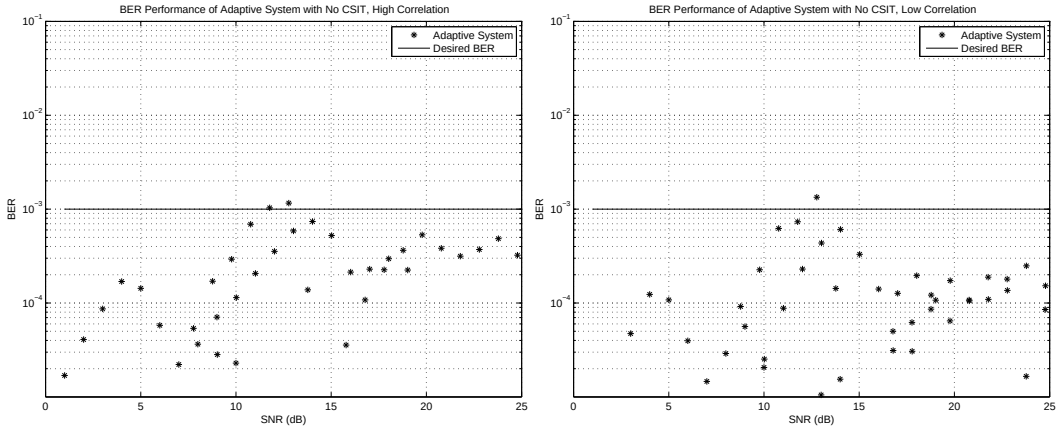

(a) High Correlation (b) Low Correlation

Figure 5.2: BERPerformance of Adaptive MIMO without CSIT

In Figure 5.2, the error performance of this adaptive system is shown. From the figure, we can see that the metrics allow the adaptive algorithm to do a very good job of meeting the desired BER for all but a small region of SNR in both the high and low spatial correlation regimes. With high correlation, the algorithm is somewhat pessimistic with low SNR leading to a much lower BER than required, which corresponds to the region where the capacity of the adaptive system is furthest from the channel capacity. With lower spatial correlation, the algorithm is somewhat pessimistic at both high and low levels of SNR, again corresponding

to larger differences between channel capacity and achieved capacity. These effects are most likely due to a limited number of constellations and code rates that were considered and would improve with a greater number of MoDem and CoDec options than were implemented.

5.3 TX Selection and Variable-Rate Multiplexing

When the feedback information is increased, handling transmitter selection information as well, the granularity between full diversity and full multiplexing systems is increased. Transmitter selection information allows the use, not just of transmit selection diversity, but also of reduced-rate multiplexing schemes.

First, Monte-Carlo simulations were again used to find the multiplexing diversity distances for each combination of array size, code rate and range of spatial correlation. The tables generated for reduced-rate multiplexing now accompany those previously found for full multiplexing.

Table 5.6: Uncoded Diversity Distance, BLAST, 10^{-3}

$N_t x N_r, Sub-streams$	$0.90 \geq \rho > 0.70$	$0.70 \geq \rho > 0.5$	$0.5 \geq \rho$
$2x2, 2$	3	2.1	1.5
$4x4, 2$	0.3	0.35	0.4
$4x4, 3$	0.7	0.7	0.7
$4x4, 4$	4	2.8	2

Table 5.7: Spatial Codeword Diversity Distance, 4x4, BLAST, 2 Sub-streams, 10^{-3}

R_c	$0.95 \geq \rho > 0.75$	$0.75 \geq \rho > 0.5$	$0.5 \geq \rho$
$\frac{3}{4}$	3	2.25	1.5
$\frac{2}{3}$	3	2.5	2
$\frac{1}{2}$	4	3	2
$\frac{1}{3}$	6	4	2.5
$\frac{1}{4}$	8	5	3
$\frac{1}{6}$	10	6	3

Table 5.8: Spatial Codeword Diversity Distance, 4x4, BLAST, 3 Sub-streams, 10^{-3}

R_c	$0.95 \geq \rho > 0.75$	$0.75 \geq \rho > 0.5$	$0.5 \geq \rho$
$\frac{3}{4}$	1.25	1.25	1.25
$\frac{2}{3}$	1.5	1.3	1.25
$\frac{1}{2}$	2	1.6	1.25
$\frac{1}{3}$	2	1.7	1.5
$\frac{1}{4}$	2	1.7	1.5
$\frac{1}{6}$	2	1.7	1.5

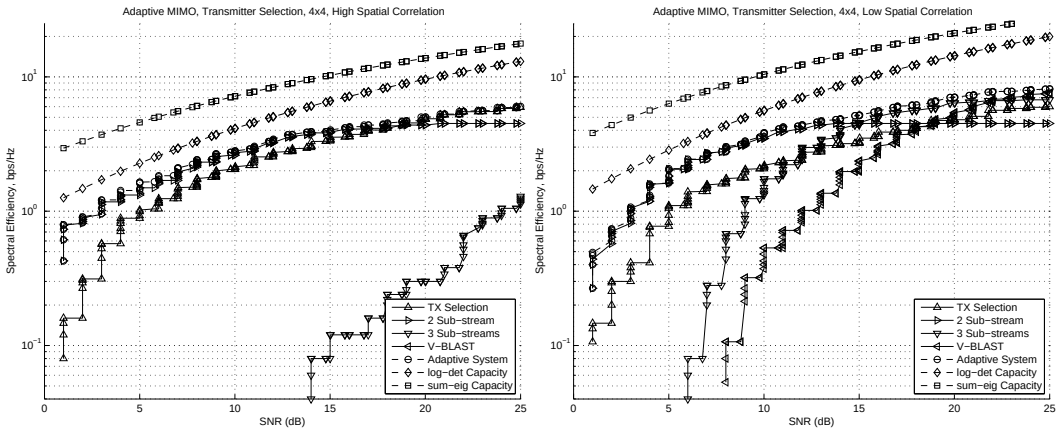

(a) High Correlation (b) Low Correlation

Figure 5.3: Performance of Adaptive MIMO with Partial CSIT

With the new reduced-rate multiplexing, the system is able to 'surf' over the four curves of capacity from each of the MIMO schemes. From Figure 5.3, it is interesting to note that under high correlation, the 2 sub-stream approach is able to come closest to the channel curve since the channel isn't yet completely rank deficient. Also, it is important to note that while the standard log-det formula for MIMO capacity was used for comparison, this assumption is not fully accurate since the feedback of transmitter selection data, carries with it implicit information about the channel back to the transmitter, thus some level of CSIT is present thereby enabling a level of power allocation across the transmit elements. For this reason, we have also included the MIMO capacity for systems with full CSIT for another means of comparison since the actual MIMO capacity for systems with partial CSIT would lie somewhere between the log-det capacity and the capacity for MIMO with full CSIT. It should be noted that while the difference between the two MIMO channel capacities is at its

greatest at low SNRs, the two channel capacities tend to converge at high SNRs, above the region shown here.

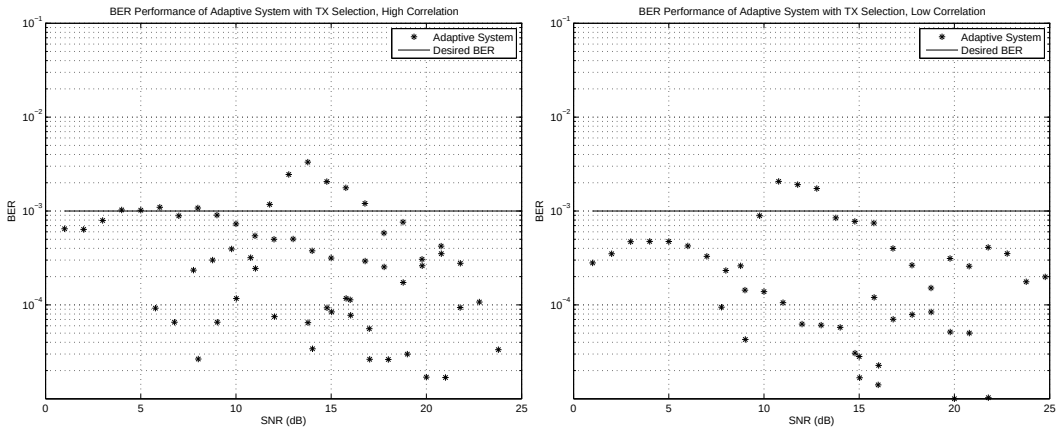

(a) High Correlation (b) Low Correlation

Figure 5.4: BER Performance of Adaptive MIMO with Partial CSIT

Figure 5.4 shows the error rate performance for the adaptive system with transmitter selection and reduced rate spatial multiplexing. For this system, the metrics enable the adaptive algorithm to perform very well, only exceeding the desired BER in a small region in both high and low spatial correlation regimes. For both high and low correlation, the adaptive system performs very close to the desired BER over the broad range of SNR values.

5.4 Variable-Rate, Eigenmode Multiplexing

Finally, with full CSIT, beamforming and eigenmode multiplexing are enabled and the multiplexing diversity distances must again be found through Monte-Carlo simulation. One

distinguishing feature of eigenmode multiplexing over BLAST is that the lack of interference between sub-streams leads to the requirement only of finding the multiplexing diversity distances for coded systems since the smallest eigenmode used will contribute the overwhelming majority of errors when uncoded and thus leads to a very tight approximation.

Table 5.9: Spatial Codeword Diversity Distance, 2x2, SVD, 2 Sub-streams, 10^{-3}

R_c	$0.90 \geq \rho > 0.70$	$0.70 \geq \rho > 0.5$	$0.5 \geq \rho$
$\frac{3}{4}$	3	2	1.5
$\frac{2}{3}$	3	2	1.5
$\frac{1}{2}$	10	4	2
$\frac{1}{3}$	10	5	2
$\frac{1}{4}$	12.5	5.5	2
$\frac{1}{6}$	15	6.5	3

In Figure 5.5, the adaptive scheme for the system with full CSIT is shown 'surfing' the capacities of all the configurations. Here, the MIMO capacity for systems with CSIT is used, for comparison. It should be noted that while CSIT does allow for the allocation of transmitted power across the eigenmodes according to their eigenvalues or spatial, it was originally decided for this work to keep the structure of the system the same as channel knowledge was varied. Consequently, the same constellation is used for each sub-stream and the use of spatial waterfilling would result in the weakest eigenmodes receiving less power

Table 5.10: Spatial Codeword Diversity Distance, 4x4, SVD, 2 Sub-streams, 10^{-3}

R_c	$0.95 \geq \rho > 0.75$	$0.75 \geq \rho > 0.5$	$0.5 \geq \rho$
$\frac{3}{4}$	1.5	1.4	1.25
$\frac{2}{3}$	1.5	1.4	1
$\frac{1}{2}$	1.5	1.4	1
$\frac{1}{3}$	2	1.6	1
$\frac{1}{4}$	2.5	1.8	1
$\frac{1}{6}$	6	4	1

Table 5.11: Spatial Codeword Diversity Distance, 4x4, SVD, 3 Sub-streams, 10^{-3}

R_c	$0.95 \geq \rho > 0.75$	$0.75 \geq \rho > 0.5$	$0.5 \geq \rho$
$\frac{3}{4}$	3	2.8	2.5
$\frac{2}{3}$	3	2.8	2
$\frac{1}{2}$	6	4.5	2
$\frac{1}{3}$	31	22	3
$\frac{1}{4}$	100	65	3
$\frac{1}{6}$	100	70	3.5

Table 5.12: Spatial Codeword Diversity Distance, 4x4, SVD, 4 Sub-streams, 10^{-3}

R_c	$0.95 \geq \rho > 0.75$	$0.75 \geq \rho > 0.5$	$0.5 \geq \rho$
$\frac{3}{4}$	3	2.7	2.5
$\frac{2}{3}$	30	12	4
$\frac{1}{2}$	60	14	3
$\frac{1}{3}$	300	63	6
$\frac{1}{4}$	1000	85	12
$\frac{1}{6}$	10000	120	12

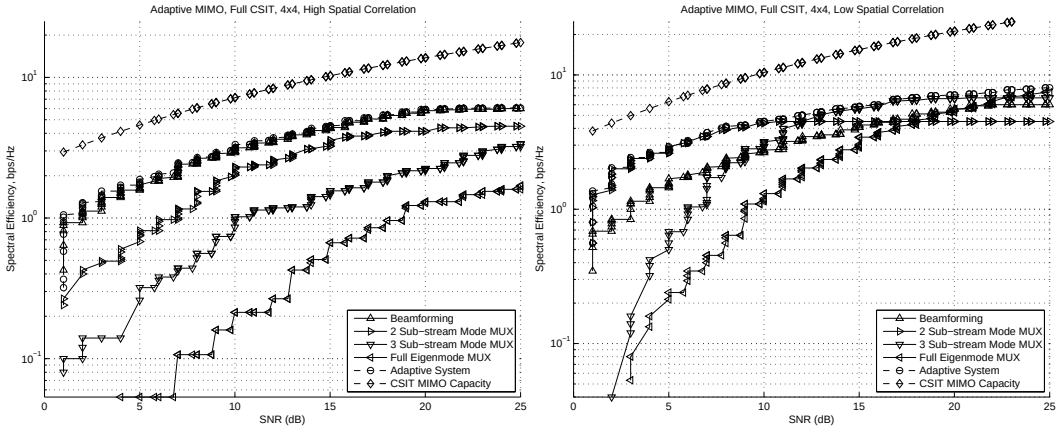

(a) High Correlation (b) Low Correlation

Figure 5.5: Performance of Adaptive MIMO with CSIT

and compounding the error dominating effect of the sub-streams transmitted on the weakest eigenmodes. With bit-loading or the use of different constellations for each sub-stream, spa-

tial waterfilling would also greatly improve the performance of a system with full CSIT. The system shown here uses equal power with equal-sized constellations for each sub-stream and uses the decoupled and interference-free nature of the eigenmodes to improve performance over the previous two systems. Again, it can be seen that the combined MoDem, CoDec and MIMO distance metrics enable the adaptive algorithm to evaluate the channel realization and SNR, to determine which joint configurations of MoDem, CoDec and MIMO scheme will satisfy the operating constraint, and is then able to maximize capacity by choosing among the eligible configurations. One interesting difference in this system's performance from high to low spatial correlation is the vast improvement in the capacity for 2 $sub-stream$ multiplexing. The low correlation combined with the $4x4$ MIMO channel allows for a strong enough second eigenmode to support 2 $sub-stream$ multiplexing at low SNRs.

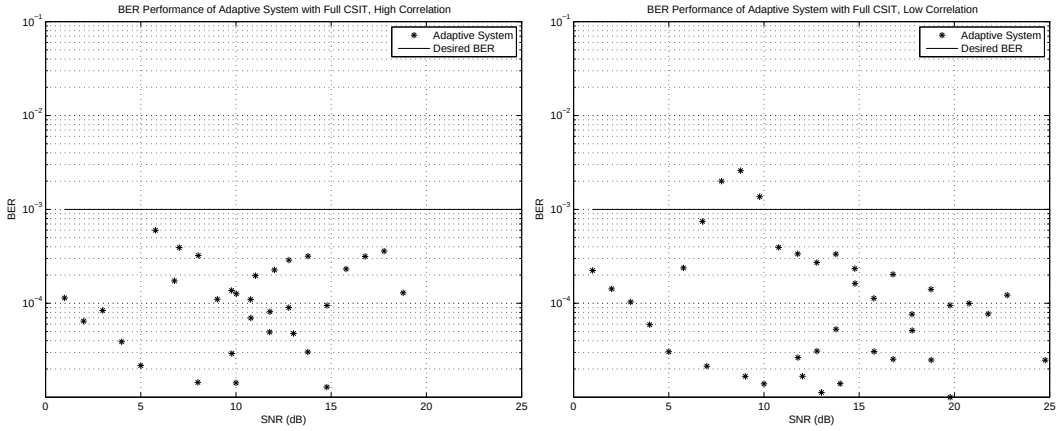

(a) High Correlation (b) Low Correlation

Figure 5.6: BER Performance of Adaptive MIMO with CSIT

Finally, in Figure 5.6, the error performance of the system with full CSIT is shown. The

system, like the one without any CSIT, is somewhat pessimistic in the highest and lowest regions of SNR, but performs very close to the desired BER on average. Again, this system would likely be able to more closely approach channel capacity and desired BER with a wider range of MoDem and CoDec options. Like the previous previous two systems, this one is also able to, on average, achieve the desired BER over a range of SNR and for high and low spatial correlation.

5.5 Rate Maximizing Adaptive MIMO Conclusions

In this chapter, the metrics and framework for adaptation of multi-antenna systems has been expanded to include the capacity maximization criteria. Additionally, a simple method for predicting the average performance of multiplexing systems using a distance factor in conjunction with a measure of the minimum eigenvalue is shown to work very well. The adaptation scheme needs only store a relatively small number of distance metrics and compute very few metrics to decide the appropriate configuration of MoDem, CoDec and MIMO scheme. Additionally, because the scheme isn't based directly on performance of simulated curves, or direct calculation of predicted BER, and the distance metrics predict average BER, they could potentially be further tuned by the radio to reflect changing requirements in the confidence that the BER for any realization of the channel will achieve the desired BER rather than in the average sense. The system is compact, flexible and attractive in terms of its minimal requirements for storage and computation.

Chapter 6

Conclusion And Future Work

6.1 Conclusion

In this work, a novel, simplified, and intuitive approach to multi-antenna adaptation has been presented. The problem of adapting multi-antenna configuration jointly with MoDem constellation and FEC CoDec has been investigated for channels of variable SNR and spatial correlation.

Two distinct regimes were studied with metrics and adaptive algorithms proposed for each. In the first, the case where a frequency-channelized network with dynamically assigned, narrow band channels is considered. On a per-antenna equal-power, equal-rate constraint and configured to achieve equal throughput to the single-band alternative, a frequency-multiplexed, parallel SISO configuration of an MTMR system is a novel approach, and shown to be able to improve energy efficiency for certain channel and network parameters.

Appropriate schedulers for the allocation of multi-antenna, multi-channel resources were developed and evaluated for both optimality of energy efficiency and computational complexity. With the developed metrics, the adaptive MTMR system is shown to have energy efficiency superior to either the Parallel SISO or the traditional, MIMO-based diversity configurations alone.

The second, more traditional regime consists of a single, spatially correlated MIMO channel and a MTMR system which has the dual goal of maximizing spectral efficiency and not exceeding a maximum tolerable BER. In addition to variable spatial correlation and SNR, the availability of CSIT, feedback capabilities and PA capabilities are considered. The final system is able to adapt to channel and system variables, meet a BER constraint and achieve spectral efficiency which follows the MIMO capacity fairly closely over a broad range of SNR.

In both halves of the proposed work, the adaptive algorithms are able to achieve their goals using a simple, compact and intuitive set of metrics.

6.2 Future Work

Once this work was completed, several areas were identified as having potential for future work in order to further improve the adaptive scheme through additional capabilities. Firstly, since the non-CSIT schemes which have been studied so far consider only the cases where all power is allocated to one transmit antenna or equally across the elements in the transmit antennas, the allocation of data bits to sub-streams or power to sub-streams with consider-

ations given to full or per sub-stream interleaving and channel coding would yield a more complete characterization and potential improvement in the efficiency of adaptive schemes. Also, since we originally did not implement spatial waterfilling for the system with full, this would be considered implemented in conjunction with bit-loading in any future work. In addition, while the $max - min$ multi-antenna, multi-channel scheduler was shown to perform well for equal-power, equal-rate, frequency multiplexing in the energy efficiency regime, the $max - max$ scheduler may become a more attractive option, when the restrictions on per-antenna, per-sub-stream for equal power and rate are removed.

The work presented here only deals with the common quasi-static, block fading model. While this model is common and easier to characterize than a fast-fading model, it does not represent a complete scenario that an actual system might encounter in the real world. To reach a more complete and realistic perspective, a fast-fading model should be adopted and studied. In addition to the factors considered for slow-fading, performance will then also depend on the length of the codeword relative to the fading speed. Additionally, with fast fading, it would also be reasonable to investigate space-time waterfilling as a way to further improve performance.

Next, the impact of a multi-user network would need to be considered. While this is more of an entire research topic unto itself, the initial investigation could begin as a continuation of this work in the context of multi-user interference, augmentation of the metrics and an investigation of the robustness of the adaptive algorithms in the presence of interference. Also, in the context of multi-user, multi-flow networks, the individual node becomes but a

single relay in the fabric through which data flows from source to destination. In this light, the traditional capacity-diversity trade off transforms into a capacity-diversity-connectivity trade off in which a single, multi-antenna node may maintain more than one simultaneous link, capable of handling simultaneous, multiple flows with resources allocated amongst them.

Ultimately, this work is but a framework for the eventual and inevitable integration into a cognitive, network-deployed system. The rules developed here, in addition to the augmentations made by multi-user investigations will provide a collection of metrics which will act as a sort of inner-loop for configuration adaptation to operate within a longer-term, outer-loop of learning and pattern recognition. Together, the framework of rules and metrics, combined with the learning capabilities of a cognitive engine will lead to the superior performance of multi-antenna radios in the real world. While the rules and metrics will provide a context for learning more quickly and adapting the system to the particulars of its surroundings, they will also provide a kind of safety net for the system, should the environment undergo radical and/or uncharacteristic changes to which the cognitive engine has not been exposed. It is the hope that this work will lead to radios that once deployed, will learn more quickly in the field than what could could be 'taught' at the factory, and that they will achieve performance superior in actual use than what can be simulated in the lab.

Appendix A

ZF alg. in [42]

1. Initialization

$$\text{(a)}\ \ i \leftarrow 1$$

$$\text{(b)}\ \ \mathbf{G}_1 = \mathbf{H}^+$$

$$\text{(c)}\ \ k_1 = \arg\min_j \parallel (\mathbf{G}_1)_j \parallel^2$$

2. Recursion

$$\text{(a)}\ \ \mathbf{w}_{k_i} = (\mathbf{G}_i)_{k_i}$$

$$\text{(b)}\ \ a_{k_i} = \mathbf{w}_{k_i}^T \mathbf{y}_i$$

$$\text{(c)}\ \ \hat{s}_{k_i} = Q(a_{k_i})$$

$$\text{(d)}\ \ \mathbf{y}_{i+1} = \mathbf{y}_i - \hat{s}_{k_i}(\mathbf{H})_{k_i}$$

$$\text{(e)}\ \ \mathbf{G}_{i+1} = \mathbf{H}_{\overline{k_i}}^+$$

$$\text{(f)}\ \ k_{i+1} = \arg \min_{j \notin \{k_1 \cdots k_i\}} \parallel (\mathbf{G}_{i+1})_j \parallel^2$$

$$\text{(g)}\ \ i \leftarrow i + 1$$

MMSE alg. in [24]

1. Initialization

$$\text{(a)}\ \ i \leftarrow 1$$

(b) $\mathbf{G}_1 = \mathbf{H}^\dagger(\mathbf{H}\mathbf{H}^\dagger + \sigma^2\mathbf{I}_{N_r})^{-1}$

(c) $k_1 = \arg\min_j \parallel (\mathbf{G}_1)_j \parallel^2$

2. Recursion

(a) $\mathbf{w}_{k_i} = (\mathbf{G}_i)_{k_i}$

(b) $a_{k_i} = \mathbf{w}_{k_i}^T \mathbf{y}_i$

(c) $\hat{s}_{k_i} = Q(a_{k_i})$

(d) $\mathbf{y}_{i+1} = \mathbf{y}_i - \hat{s}_{k_i}(\mathbf{H})_{k_i}$

(e) $\mathbf{G}_{i+1} = \mathbf{H}_{\overline{k_i}}^\dagger(\mathbf{H}_{\overline{k_i}}\mathbf{H}_{\overline{k_i}}^\dagger + \sigma^2\mathbf{I}_{N_r})^{-1}$

(f) $k_{i+1} = \arg\min_{j \notin \{k_1 \cdots k_i\}} \parallel (\mathbf{G}_{i+1})_j \parallel^2$

(g) $i \leftarrow i + 1$

Bibliography

[1] E. Al-Hussaini and A. Al-Bassiouni. Performance of MRC diversity systems for the detection of signals with nakagami fading. *Communications, IEEE Transactions on*, 33(12):1315–1319, Dec 1985.

[2] S. Alamouti. A simple transmit diversity technique for wireless communications. *Selected Areas in Communications, IEEE Journal on*, 16(8):1451–1458, October 1998.

[3] R. Buehrer. Generalized equations for spatial correlation for low-to-moderate angle spread. In *Virginia Tech Symposium on Wireless Personal Communications, 2000. Proceedings. 10th*, pages 123–130, June 2000.

[4] A. Calderbank, N. Seshadri, and V. Tarokh. Space-time codes for wireless communication. In *Information Theory. 1997. Proceedings., 1997 IEEE International Symposium on*, pages 146–, June - July 1997.

[5] S. Catreux, V. Erceg, D. Gesbert, and J. Heath, R.W. Adaptive modulation and MIMO coding for broadband wireless data networks. *Communications Magazine, IEEE*, 40(6):108–115, Jun 2002.

[6] F. Farrokhi, G. Foschini, A. Lozano, and R. Valenzuela. Link-optimal BLAST processing with multiple-access interference. In *Vehicular Technology Conference, 2000. IEEE VTS-Fall VTC 2000. 52nd*, volume 1, pages 87–91, 2000.

[7] A. Forenza, M. McKay, I. Collings, and R. Heath. Switching between OSTBC and spatial multiplexing with linear receivers in spatially correlated MIMO channels. In *Vehicular Technology Conference, 2006. VTC 2006-Spring. IEEE 63rd*, volume 3, pages 1387–1391, May 2006.

[8] A. Forenza, M. McKay, A. Pandharipande, R. Heath, and I. Collings. Adaptive MIMO transmission for exploiting the capacity of spatially correlated channels. *Vehicular Technology, IEEE Transactions on*, 56(2):619–630, March 2007.

[9] A. Forenza, A. Pandharipande, H. Kim, and J. Heath, R.W. Adaptive MIMO transmission scheme: Exploiting the spatial selectivity of wireless channels. In *Vehicular Technology Conference, 2005. VTC 2005-Spring. 2005 IEEE 61st*, volume 5, pages 3188–3192, May - June 2005.

[10] G. Foschini, G. Golden, R. Valenzuela, and P. Wolniansky. Simplified processing for high spectral efficiency wireless communication employing multi-element arrays. *Selected Areas in Communications, IEEE Journal on*, 17(11):1841–1852, November 1999.

[11] G. J. Foschini. Layered space-time architecture for wireless communication in a fading environment when using multi-element antennas. *Bell Labs Technical Journal*, 1(2):41–59, 1996.

[12] G. J. Foschini and M. J. Gans. On limits of wireless communications in a fading environment when using multiple antennas. *Wireless Personal Communications*, 6(3):311–335, March 1998.

[13] G. Ganesan and P. Stoica. Space-time block codes: a maximum SNR approach. *Information Theory, IEEE Transactions on*, 47(4):1650–1656, May 2001.

[14] G. Golden, C. Foschini, R. Valenzuela, and P. Wolniansky. Detection algorithm and initial laboratory results using V-BLAST space-time communication architecture. *Electronics Letters*, 35(1):14–16, Jan 1999.

[15] S. Haykin and M. Moher. *Modern Wireless Communication*. Prentice-Hall, Inc., Upper Saddle River, NJ, USA, 2004.

[16] R. Heath and A. Paulraj. Switching between diversity and multiplexing in MIMO systems. *Communications, IEEE Transactions on*, 53(6):962–968, June 2005.

[17] W. C. Jakes and D. C. Cox, editors. *Microwave Mobile Communications*. Wiley-IEEE Press, 1974.

[18] I. Kim, K. Lee, and J. Chun. A MIMO antenna structure that combines transmit beamforming and spatial multiplexing. *Wireless Communications, IEEE Transactions on*, 6(3):775–779, March 2007.

[19] N. Kita, W. Yamada, A. Sato, D. Mori, and S. Uwano. Measurement of demmel condition number for 2x2 MIMO-OFDM broadband channels. In *Vehicular Technology*

Conference, 2004. VTC 2004-Spring. 2004 IEEE 59th, volume 1, pages 294–298, May 2004.

[20] S. Le Goff, A. Glavieux, and C. Berrou. Turbo-codes and high spectral efficiency modulation. In *Communications, 1994. ICC '94, SUPERCOMM/ICC '94, Conference Record, 'Serving Humanity Through Communications.' IEEE International Conference on*, volume 2, pages 645–649, May 1994.

[21] J. R. Lee and M. H. Ahmed. A-BLAST: A novel approach to adaptive layered space-time processing. In *IWCMC '06: Proceedings of the 2006 international conference on Wireless communications and mobile computing*, pages 659–664, New York, NY, USA, 2006. ACM.

[22] W. C. Y. Lee. *Mobile Cellular Telecommunications Systems.* McGraw-Hill, Inc., New York, NY, USA, 1990.

[23] X.-B. Liang. Orthogonal designs with maximal rates. *Information Theory, IEEE Transactions on*, 49(10):2468–2503, October 2003.

[24] H. Matsuda, K. Honjo, and T. Ohtsuki. Signal detection scheme combining MMSE V-BLAST and variable K-best algorithms based on minimum branch metric. In *Vehicular Technology Conference, 2005. VTC-2005-Fall. 2005 IEEE 62nd*, volume 1, pages 19–23, September 2005.

[25] M. McKay, I. Collings, A. Forenza, and R. Heath. Multiplexing/beamforming switching for coded MIMO in spatially correlated channels based on closed-form BER approxi-

mations. *Vehicular Technology, IEEE Transactions on*, 56(5):2555–2567, September 2007.

[26] R. Narasimhan. Spatial multiplexing with transmit antenna and constellation selection for correlated MIMO fading channels. *Signal Processing, IEEE Transactions on*, 51(11):2829–2838, November 2003.

[27] J. G. Proakis and M. Salehi. *Digital Communications*. McGraw Hill Higher Education, 5th edition, January 2008.

[28] L. Qiang, D. Peng, and B. Guangguo. Generalized soft decision metric generation for MPSK/MQAM without noise variance knowledge. In *Personal, Indoor and Mobile Radio Communications, 2003. PIMRC 2003. 14th IEEE Proceedings on*, volume 2, pages 1027–1030, September 2003.

[29] T. S. Rappaport and T. Rappaport. *Wireless Communications: Principles and Practice (2nd Edition)*. Prentice Hall PTR, December 2001.

[30] N. Seshadri, V. Tarokh, and A. Calderbank. Space-time codes for wireless communication: code construction. In *Vehicular Technology Conference, 1997 IEEE 47th*, volume 2, pages 637–641, May 1997.

[31] P. Smith, M. Shafi, and L. Garth. Performance analysis for adaptive MIMO SVD transmission in a cellular system. In *Communications Theory Workshop, 2006. Proceedings. 7th Australian*, pages 49–54, February 2006.

[32] R. Steele. *Mobile Radio Communications*. John Wiley & Sons, Inc., New York, NY, USA, 1999.

[33] W. Su, X.-G. Xia, and K. Liu. A systematic design of high-rate complex orthogonal space-time block codes. *Communications Letters, IEEE*, 8(6):380–382, June 2004.

[34] V. Tarokh, H. Jafarkhani, and A. Calderbank. Space-time block codes from orthogonal designs. *Information Theory, IEEE Transactions on*, 45(5):1456–1467, Jul 1999.

[35] V. Tarokh, H. Jafarkhani, and A. Calderbank. Space-time block coding for wireless communications: performance results. *Selected Areas in Communications, IEEE Journal on*, 17(3):451–460, March 1999.

[36] V. Tarokh, A. Naguib, N. Seshadri, and A. Calderbank. Combined array processing and space-time coding. *Information Theory, IEEE Transactions on*, 45(4):1121–1128, May 1999.

[37] V. Tarokh, N. Seshadri, and A. Calderbank. Space-time codes for high data rate wireless communication: performance criterion and code construction. *Information Theory, IEEE Transactions on*, 44(2):744–765, March 1998.

[38] E. Telatar. Capacity of multi-antenna gaussian channels. *European Transactions on Telecommunications*, 10:585–595, 1999.

[39] M. Vu and A. Paulraj. MIMO wireless linear precoding. *Signal Processing Magazine, IEEE*, 24(5):86–105, September 2007.

[40] H. Wang and X.-G. Xia. Upper bounds of rates of complex orthogonal space-time block codes. *Information Theory, IEEE Transactions on*, 49(10):2788–2796, October 2003.

[41] M. Wang, W. Xiao, and T. Brown. Soft decision metric generation for QAM with channel estimation error. *Communications, IEEE Transactions on*, 50(7):1058–1061, July 2002.

[42] P. Wolniansky, G. Foschini, G. Golden, and R. Valenzuela. V-BLAST: An architecture for realizing very high data rates over the rich-scattering wireless channel. In *Signals, Systems, and Electronics, 1998. ISSSE 98. 1998 URSI International Symposium on*, pages 295–300, September - October 1998.

[43] R. Yazdani and M. Ardakani. Optimum linear LLR calculation for iterative decoding on fading channels. In *Information Theory, 2007. ISIT 2007. IEEE International Symposium on*, pages 61–65, June 2007.

[44] Z. Zhou, B. Vucetic, M. Dohler, and Y. Li. MIMO systems with adaptive modulation. *Vehicular Technology, IEEE Transactions on*, 54(5):1828–1842, Sept. 2005.

[45] H. Zhuang, L. Dai, S. Zhou, and Y. Yao. Low complexity per-antenna rate and power control approach for closed-loop V-BLAST. *Communications, IEEE Transactions on*, 51(11):1783–1787, Nov. 2003.